Water-efficient Indian rice cultivation boosts exports despite high carbon footprints

Mukund Narayanan[1,2], Idhayachandhiran Ilampooranan[1]*, Peter C. McKeown[2], Ankit Sharma[1], Noel Ndlovu[2] & Charles Spillane[2]*

[1]Department of Water Resources Development and Management, Indian Institute of Technology Roorkee, Roorkee, Uttarakhand, India.
[2]Agriculture, Food Systems & Bioeconomy Research Centre, Ryan Institute, University of Galway, University Road, Galway H91 REW4, Ireland.

*Corresponding Authors:
Idhayachandhiran Ilampooranan – idhaya@wr.iitr.ac.in
Charles Spillane – charles.spillane@universityofgalway.ie

This research paper is a non-peer reviewed preprint submitted to EarthArXiv.

ORCID:

Mukund Narayanan (MN) – 0000-0001-9558-320X
Idhayachandhiran Ilampooranan (II) – 0000-0003-0819-376X
Peter C. McKeown (PM) – 0000-0002-7255-6062
Ankit Sharma (AS) – 0009-0007-4294-0753
Noel Ndlovu (NN) – 0000-0002-1832-0251
Charles Spillane (CS) – 0000-0003-0819-376X

Author Contributions:

Conceptualization – MN, II, PM, CS, & NN
Data curation – MN
Formal analysis – MN, AS, II, PM, & CS
Funding acquisition – MN, II, PM, & CS
Investigation – MN, AS, II, PM, & CS
Methodology – MN, II, PM, & CS
Project administration – II, PM, & CS
Software – MN
Resources – II, PM, & CS
Supervision – II, PM, & CS
Validation – MN, AS, II, PM, & CS
Visualization – MN, AS, II, PM, & CS
Writing - original draft – MN, AS, CS, II, NN & PM
Writing - review & editing – MN, AS, CS, II, PM, & NN

Abstract

Most agricultural sustainability efforts adopt a national-scale view, masking regional trade-offs between crop yields and environmental footprints. To measure trade-offs, satellite remote sensing based life cycle assessment of rice agroecosystems across India from 2004 to 2021 was conducted revealing pivotal shifts of four cultivation typologies, termed as unsustainable, conventional, productive, and sustainable. Over the period, sustainable and productive rice areas expanded by ~32% and ~40% respectively, while unsustainable and conventional areas declined by ~68% and ~60%. Paradoxically, the most water-efficient sustainable typology at ~339.9 mm/ha generated the largest carbon footprint at ~2066.6 kg C/ha due to residue burning. We calculate that a complete transition to sustainable cultivation could boost India's export revenues by 60% to USD 15.59 billion, while shifting to unsustainable cultivation could halve export revenues. Projections to 2031 show both sustainable and unsustainable typologies becoming dominant, covering 58% of India's rice areas, highlighting the need for region-specific policies.

Keywords: Life Cycle Assessment, Rice Cultivation, Sustainability, Rice Exports, Water Use Efficiency, Satellite remote sensing

Life Cycle Assessment (LCA) is a systematic approach for measuring the environmental footprints associated with all stages of a product, from raw material extraction through processing, manufacturing, distribution, use, and disposal[1–3]. LCA has become an increasingly useful tool worldwide to inform coherent and evidence-based solutions to environmental degradation[4], climate change[5], and resource depletion[6]. In Indian rice cultivation systems, the application of LCA is important[7,8] as India's large-scale agriculture area (in 2022-23: 47.83 million hectares (ha)[9]) contributes to substantial greenhouse gas emissions[10,11], and land degradation[12], yet is dominated by smallholders (average size ~1.08 ha[13]). Due to this, making sustainable and widespread policy recommendations such as promoting system rice intensification[14] and integrated farming systems[15] becomes challenging as income, access to information, distance market etc. may vary significantly across rice farms[16].

Indian rice cultivation feeds nearly one-seventh of the world's population (1.2 billion people) across 150 countries[17,18] and is crucial for global food security. India is currently the world's largest rice exporter, supplying ~17.83 million tonnes of rice worth 10.45 billion USD in 2023, representing 32.3% of global rice exports[19]. Rice is a key component of global diets (17.3% of total calories from rice; 516 kcal/capita/day[20]), and significantly contributes (0.73% of India's gross domestic product: ~23.24 billion USD from rice production in 2021[21]) to India's economy.

Despite the economic and nutritional importance of rice to India, the traditional flooded rice systems (requiring ~2,500 litres of water to produce a single kg[11,22]) have high environmental footprints (water, greenhouse gases, nitrogen, etc.) as they are major methane emissions sources[22,23], releasing ~3.7 to ~4.8 teragrams (Tg) of methane between 1966-2017[11]. Furthermore, the intensive and inefficient use of fertilizers[16] leads to nitrogen leaching from rice fields[10], in addition to emissions associated with fertilizer use[24].

Sustainable intensification trajectories that reduce environmental footprints while sustaining yields of rice production are necessary[25,26], where transitions to more sustainable rice cultivation can be achieved. However, this needs to be balanced with economic considerations such as commodity prices, value chain profitability, export earnings and viable household incomes for smallholder rice production. While this can be achieved through environmental footprinting of rice cultivation[27–30], most footprinting studies to date are at national or regional scales, overlooking the spatial diversity of India's 18 agro-climatic zones[31], seven rice water-regimes[32,33] and biogeochemical variability caused due to varied irrigation methods[34,35], fertilizer application rates[16], and crop residue management[16,35] .

Finer-scale LCA approaches have the potential to identify environmental hotspots and quantify footprints with greater spatial and temporal accuracy. However, achieving this depends on accurate representation of rice agroecosystem biogeochemical processes, which is becoming possible through high-resolution satellite observations and sub-national data on land use and agronomy. To our knowledge satellite data and derived products for large-scale LCA across rice fields and landscapes have not been used despite their potential in mapping rice areas and yields[36,37], monitoring methane emissions[38–40], and estimating management practices[41,42]. To address this knowledge gap, in this study we harmonize satellite, statistical, and derived datasets for a comprehensive LCA of Indian rice farming at fine scale 500 m resolution (~25 ha of area) across all rice cultivation areas of India, identifying environmental hotspots and cultivation typologies, while also analysing the impact of different cultivation typologies on export revenues for fine-scale guiding of sustainable intensification of rice production.

Results

Spatio-temporal Variation of LCA Indicators (Water, Carbon, and Nitrogen footprint) of rice production

Here we measure the environmental footprint of rice cultivation across all of India at 500 m resolution using a cradle to farmgate LCA approach, which covers sowing to harvest and input production processes (Table 1) over the period 2004 to 2021. In addition to rice yields, we also measure the water, carbon and nitrogen footprint (Fig. 1; Table S1), which are derived from the irrigation and precipitation water consumption, global warming potential, and nitrogen loss to rivers, respectively. Nationally, rice yields in India increased substantially over the 18-year period, most prominently in the traditionally high-

yielding zones of the Punjab and Haryana, which are associated with varied environmental footprints. In the Punjab region, rice cultivation areas that predominantly recorded rice yields in the ~1,450 (314-2,277) kg C/ha range in 2004 transitioned almost entirely to the highest productivity of ~1,639 (368-2,475) kg C/ha by 2021. This yield enhancement (13% increase) was however driven by a 1.2-fold increase in the water footprint, 9% surge in nitrogen footprint, and 6% increase in carbon footprint during the same period. Conversely, the Bengal region exhibited a more significant 37% yield increase, shifting from ~317 (12-1,990) kg C/ha in 2004 to ~434 (30-1,662) kg C/ha by 2021, while maintaining a consistent water (~576 (3-1,685) mm) and nitrogen footprint (~136 (107-231) kg N/ha). However, like the Punjab region, the Bengal region experienced a 11% increase in its carbon footprint. Most substantially, the Andhra region yield's increased nearly two-fold from ~553 (56-1,808) kg C/ha to ~916 (37-1,066) kg C/ha. However, this was associated with a 16% and a 9% increase in water and nitrogen footprint along with a 5% decrease in carbon footprint.

Dynamics and Drivers of Rice Production Footprints

In 2004-2021, the total annual carbon additions in rice areas diminished from 2,632.32 kg C/ha to 2,529.45 kg C/ha, while total carbon removals displayed an increasing trend from 2,239.56 kg C/ha to 2,510.39 kg C/ha (Fig. 2a). This overall carbon deficit drove a decline in soil organic carbon stocks, which fell by ~500 kg C/ha over the 18-year period. Carbon inputs were dominated by manure application (92.4%), which decreased over time. The remaining 7.6% of carbon inputs originated from the 1.5-fold increase of returning rice residue from 160 to 240 kg C/ha. Amongst the carbon removals, methane emissions (46.7%) constituted the largest pathway, declining by 16% between 2004 and 2021. However, rice yield (31.8%) and residue burning (11.7%) drove the parallel increase in total carbon removals, as their values nearly doubled during the 18-year period. In parallel, the nitrogen budget (Fig. 2b) of rice production from 2004 to 2021 (Fig. 2b) displayed an increase in total additions, which grew 33% from 124.84 kg N/ha to 166.52 kg N/ha in 2004-2021 driven by manure, fertilizer, and rice residue. In contrast, total nitrogen removals as N loss to rivers (~160 kg N/ha) rose more slowly over the same period (6% increase). In water footprints (Fig. 2c), during 2004-2021, a 10% and 23% decrease in green and blue water footprints was observed from ~500 to ~450 mm/ha and ~130 to ~100 mm/ha, respectively. These changes were driven by the 20% decline in precipitation from June-September and a 12.5% decrease in evapotranspiration. However, the halving of precipitation in October-March and evapotranspiration in April-May also contributed to the decline in water footprints, but was relatively minor due to the higher magnitude of value of June-September.

Sustainable vs Unsustainable Rice Cultivation Typologies

For analysing regional variations, the study classified Indian rice cultivation using quantile classification (Q1 to Q4) of temporally averaged normalized yields and inverse footprints (see Methods). This classification revealed four rice cultivation typologies (unsustainable (Q1), conventional (Q2), productive (Q3), and sustainable (Q4)) for each year during 2004-2021. Temporally (2004-2021; Fig. 3c), the unsustainable and conventional areas decreased from ~68% to ~60%, while sustainable and productive areas increased from ~32% to ~40%. As these typologies fluctuated across years (2004-2021) at each location (Fig. S1), our analysis used a persistence metric which represents the frequency of typology observed in each 500 m pixel expressed between zero to one, as shown in heatmaps of Fig. 3a. For example, if the rice pixel is unsustainable for six of 18 years (intermittently or sequentially), its persistence under each typology would be: 0.33 (6/18). Here, persistence values classified into five levels from very low frequency (<0.2) to very high (>0.8) frequency (Fig. 3a; Table S2). In the productive typology, Haryana and coastal deltas showed consistent above moderate persistence (>0.4) in 3.47% of Indian rice areas (Fig. 3a; Table S2). However, this typology was largely non-persistent (<0.4) across 96.53% of areas. Similarly, in the sustainable typology, most areas (83.12%) were non-persistent with exceptions (>0.6 persistence) in Punjab and the Western Ghats (12.89% of rice areas). The conventional typology across central India was highly widespread, with extensive non-persistence (95.41% of rice areas). In contrast, the unsustainable typology was heavily concentrated in northeastern India (Assam and West Bengal), with substantial above moderate persistence in 25.6% of rice areas. Further, our decadal forecasting (2022-2031; Fig. 3c) predicts that unsustainable and sustainable typologies will increase by 4% and 9% during 2022-2031 at the cost of decreasing conventional and productive typologies by 5% and 7%, respectively (Fig. 3c).

Exploring characteristics of these typologies, climatologically (Fig. 3b), rainfall was higher in the unsustainable (163.6 mm) and conventional (120.5 mm) typologies than in the productive (106.4 mm)

and sustainable (75.2 mm) typologies (Fig. 3b). Also, the sustainable and productive typologies experienced higher windspeeds of 3.3 m/s and 2.8 m/s, possibly explaining their ~9% higher evapotranspiration. In agronomic management practices (Fig. 3b), the sustainable typology was the most intensive, while having the highest yield (3,369 kg/ha) and the lowest nitrogen and water footprints (135 kg N/ha and 339.9 mm/ha), with the highest fertilizer rate (264.3 kg/ha), seed rate (2.3 kg/ha), and ground water depth (4.4 m). Moreover, the sustainable typology was associated with the most alkaline soil (pH 7.5) and the largest carbon footprint (2,066.6 kg C/ha), while having the lowest soil organic carbon and total nitrogen values (1.7% and 1.5%). This typology was considered sustainable as it has the highest overall footprint use efficiency (total footprints per unit rice yield) (Table S3). Conversely, the unsustainable typology produced the lowest yield (1,057.4 kg/ha), fertilizer input (111.5 kg/ha) and pH (6.5), but had the highest soil organic carbon (2.2%), total nitrogen (2.0%), nitrogen footprint (140.9 kg N/ha) and water footprint (685.8 mm/ha) values. Intermediate to the unsustainable and sustainable typologies, the productive and conventional typologies generated yields of 1,932.3 kg/ha and 1,412.2 kg/ha with 183.5 kg/ha and 154.6 kg/ha of fertilizer, respectively.

Economic growth and environmental footprint flows in rice exports from India

Our export analysis investigated changes in economic value and environmental footprint flows from Indian rice exports under complete typology transitions (Fig. 4; Table S3). In 2004, the sustainable typology secured the highest trade value (~2.78 billion USD) relative to the base case (~1.18 billion USD). Conversely, the conventional typology generated the lowest initial trade value (2004: 0.51 billion USD), while the unsustainable and productive typologies produced revenues notably lower than the base case (35% and 17% lower). By 2021, the sustainable typology maintained the leading position with increased revenues (~15.59 billion USD) relative to the base case (~9.62 billion USD). Following this, the productive typology significantly surpassed the baseline to achieve a greater economic return (11.76 billion USD) which reflected an increase. Although showing growth (6.16 and 4.92 billion USD) in 2021, the conventional and unsustainable typologies remained 36% and 51% less than the base case revenue. Between 2004 and 2021, the geographical distribution of environmental footprints of India's rice exports shifted from Saudi Arabia to Bangladesh, Nepal, and Benin. During this period, the sustainable and productive typologies involved a maximum flow to 22 and 16 trade partners in the low impact category (vs. 16 in base case) (Fig. 4b,c,d). Specifically, the trade partners under these typologies were low in carbon (<0.25 million tons), nitrogen (<25 thousand tons), and water footprint (<250 MCM) flows relative to other countries. Moreover, these typologies also had less than 12 trade partners in the upper 5% of footprints flows (Table S3). In contrast, the unsustainable and conventional typologies had 21 and 19 countries in the upper 5% of footprint flows (Table S3), while having less than 12 low impact trade partners (Fig. 4b,c,d).

Discussion

Policy-driven rice yield intensification increases environmental footprints

Indian rice cultivation from 2004 to 2021 underwent distinct regional variations in yields, and associated water, carbon, and nitrogen footprints (Fig. 1a-h), possibly driven by adoption of higher yielding varieties and nutrient subsidies[43–45]. Over this period, rice yields increased nationwide, with the most significant gains in the Andhra Region and the Bengal Region. This yield gain is linked to the adoption of high-yielding hybrid varieties and intensive fertilizer use[46]. For instance, ICAR-NRRI[47] developed three popular hybrids, Ajay, Rajalaxmi, and CR Dhan 701, which demonstrate 20-30% more yield than traditional varieties. Further, the introduction of Nutrient Based Subsidy (NBS) scheme for phosphatic, potassic, and urea fertilizers has made nitrogen fertilizers more affordable, encouraging more usage[48]. However, this policy-driven intensification of rice yields has likely exacted a considerable environmental footprint. For example, the carbon footprint was highest in the Punjab region due to residue burning practices[49]. Similarly, subsidized electricity and guaranteed procurement prices[43] encouraged extensive groundwater irrigation for water-intensive practices like continuous flooding, which may have led to the observed 1.3-fold increase of water footprint in the Punjab and Andhra region during 2004-2021. Moreover, over irrigation driven by farm subsidies, has depleted ground water levels in Punjab[43] and Telangana[50]. Simultaneously, the use of higher yielding varieties in these regions and could have increased the nitrogen footprint due to the high fertilizer demands of modern cultivars (~248 kg N/ha[47]).

However, further substantiation regarding the nitrogen demands in high yield varieties at regional scale is needed as hybrid rice varieties can be more nitrogen-use efficient and tolerant of low-nitrogen conditions than traditional rice. In the Bengal region, there was a yield increase observed while maintaining a stable water footprint suggesting that regional management practices, such as managing irrigation timing against rainfall could decouple yield gains from environmental impacts[51]. Nevertheless, the nitrogen and carbon footprint in the Bengal region nearly doubled during the period 2004-2021, likely driven by nutrient subsidies for urea from the NBS scheme and rice methane emissions[11]. These findings highlight how policies enhanced yields but increase environmental footprints, necessitating region-specific sustainable (more yield and less footprint) management strategies.

Dynamics and drivers of the environmental footprints of Indian rice cultivation

During 2004-2021, the India-scale rice cultivation carbon dynamics indicate a decline in soil organic carbon stocks that appears to be driven by increases in carbon removals and decreases in carbon additions. This carbon removals was influenced by the increase of rice residue burning, although rice methane emissions remained the largest pathway. The short time gap (10-20 days) for land preparation between the rabi (October-April) and the kharif (June-September) seasons is the primary reason for the rice straw burning practices[52]. Importantly, the rice residue removal does not return as much revenue as it cannot be used as livestock fodder due to high silica content[53,54]. Unlike the carbon removals, between 2004-2021 carbon additions decreased due to the reduction of the livestock population in the period[56]. This was because manure is the most dominant carbon addition and livestock population determines how much manure is added to the field[11]. In nitrogen dynamics, while agricultural subsidies that incentivized increased fertilizer application[57] increased nitrogen additions, a disconnected slower increase in nitrogen removals suggests a slightly declining nitrogen use efficiency in the rice cultivation system. This may be due to biological advancements (e.g., screening nitrogen efficient genotypes[58] and biofortification[59]) in increasing the rice crop's nitrogen uptake under intensive management regimes. However, this disconnect between nitrogen additions and removals may also be a result precipitation driven nitrogen loss[60]. In the water footprint dynamics, while reduced water footprints appear to indicate improved water use efficiencies, they are speculated to have actually masked underlying processes such as ground water extraction that threaten long-term agricultural sustainability[61]. For instance, between 2004-2015 the groundwater table depth across rice-growing areas in India increased from 3.96 m to 4.23 m[62], indicating continued groundwater depletion despite the reduction in the overall water footprint. This was because the blue water footprint metric reflects the volumetric irrigation demand without identifying the specific origin of water sources (surface or ground water). As a result, lower water footprints values create a false signal of improved efficiency. Due to this, climate adaptive water management strategies such as alternate wetting and drying to maintain crop productivity are necessary[63].

Spatiotemporal variations of rice cultivation typologies

The temporal changes of rice cultivation typologies from 2004 to 2021 are reflective of policy interventions promoting sustainable agriculture driven by hybrid variety adoption and nutrient subsidies[43–45] and a declining reliance on unsustainable practices. For instance, the concentration of the productive typology in northwestern regions (e.g. Haryana) and the sustainable typology (in Punjab) demonstrates how modern high-yielding rice varieties contribute to more intensive cultivation patterns that maximize productivity[64] with minimal environmental impact. However, the geographic concentration of the unsustainable typology in eastern regions (West Bengal and Assam) and conventional typology in central India (Chhattisgarh and Bihar) reflects historical cultivation patterns in flood-prone environments which generate high methane emissions, increasing both water and carbon footprints[65], while providing marginal yields. The lower water footprint and higher yield in the sustainable typology cultivation, when compared to the unsustainable typology, underscore how irrigation management practices coupled with increased yields can provide routes to more sustainable intensification[66]. However, it could be considered that the sustainable typology in the aggregate is masking situations where the carbon footprints are relatively higher due to crop residue burning, creating a trade-off whereby significant carbon emissions undermine gains in water conservation.

The reduction in rice residue burning can enhance the sustainability (high yield and low carbon, nitrogen, and water footprints) of the sustainable typology significantly. The projected future increase of the sustainable typology reflects policy momentum in India (e.g., National Mission on Sustainable

Agriculture[67]) toward climate-smart agriculture in response to food security and environmental degradation concerns[68]. In parallel, future increases in the unsustainable typology could arise due to soil alkalinization associated with continuous flooding and high nitrogen inputs[69]. While the sustainable and unsustainable typologies increase over time, their high persistence is concentrated in only a few regions across India (<8% of areas; Fig. 3), indicating that rice cultivation in most of India experiences these patterns only temporarily. This raises the possibility of restoration of rice-growing areas under the unsustainable typology under good agronomic management, and possible degradation of sustainable typology under poor agronomic management. Therefore, focusing on how to maintain and ensure transitions towards sustainable typologies of rice production in India is of paramount importance.

Implications of Environmental Footprints embedded in Rice Exports

The variations in typologies of rice cultivation in India have significant economic and trade implications (Fig 4a), through generation of environmental footprints (Fig 4b-d) which are subsequently embedded in India's rice exports to global trade partners. For instance, the sustainable typology proved most efficient because it generated the highest revenue with significantly lower footprint flows relative to the base case. In contrast, the unsustainable typology had the greatest inefficiency by producing disproportionately large environmental footprint flows for the lowest economic gain. If the environmental footprints of India's rice production are not managed, there is potential that trading partners may reduce their imports of high environmental footprint rice from India and conversely favour imports of lower environmental footprint rice. Such a scenario could significantly impact India's revenue as rice exports contribute ~0.4% of national GDP[19]. Transitioning to lower environmental footprint rice cultivation typologies is desirable, but will require integrated approaches that can lever innovations across biological, geographical, and labour dimensions. Biologically, advances in rice breeding can generate higher yielding varieties with greater resource use (e.g. water, nitrogen) efficiency to increase the sustainability of Indian rice cultivation. For instance, farmers could consider adopting the newly released genome edited rice (DRR Rice 100 (Kamla) and Pusa DST Rice 1) by the Ministry of Agriculture & Farmers Welfare[70] which consumes less water, reduces greenhouse gas emission by 20%, and produces 19% higher yields. Other rice genetics innovations that can be considered are deployment of drought tolerant rice varieties (e.g. Sahbhagi Dhan[71]) and submergence/flood tolerant (Sub1) varieties[72]. On the geographic front, strategic relocation of rice cultivation based on biophysical suitability parameters offers opportunities for sustainable intensification through geographic specialization aligned with natural resource availability[73]. Such relocation approaches can involve identification suitable zones with adequate rainfall, appropriate temperatures, and clayey soils that naturally support rice cultivation with minimal environmental footprints. In addition, labour availability is a critical constraint requiring specific attention in sustainability transition strategies. The declining agricultural workforce (e.g. from 63% to 44% of total employment in India during 1991-2023[74]) indicates that mechanization is a key strategy for maintaining and increasing rice production capacity in India while compensating for reduced labour availability[75]. The integrated deployment and scaling of such innovations will likely need to be a key feature of pathways for improving sustainability of rice cultivation in India. However, more studies which focus on water regime specific (irrigated vs. rainfed) policy recommendations may be beneficial during final implementation of these innovations. In conclusion, regional trade-offs between rice yields and environmental footprints were quantified at a fine scale 500 *m* resolution across India from 2004 to 2021. Our analysis reveals that the high yielding and low water footprint sustainable typology of rice cultivation in India generates large carbon footprints because of rice residue burning practices. While transitioning to this sustainable typology increases export revenues by 60% to 15.59 billion USD, it also requires addressing trade-offs with increased emissions.

Methods

System Boundary

This satellite-based LCA framework primarily defines the spatial system boundary through rice cultivation areas that were identified and mapped using Moderate Resolution Imaging Spectroradiometer (MODIS) data. Specifically, MODIS Terra satellite eight-day surface reflectance data (MOD09A1.061) at a 500 *m* resolution. The assessment framework also standardizes various environmental and agricultural variables into specific functional units. The functional units of all variables are listed in Table 1.

Temporal Scope

To capture all stages and activities directly involved in the production of rice, the system boundary set in this LCA is from sowing/transplantation to harvesting of the rice crop in the fields across a temporal range from 2004 to 2021. This period encapsulates the critical biological growth phase of the rice plant and the associated on-field management activities, including seeding, irrigation water, machinery usage, nutrient application, and pest control, which are the direct control points for farmers. In addition to this, footprints of inputs such as fertilizer production, irrigation pumping fuel and electricity, seed production, and pesticide production are added to the above system (Fig. S2). Although these additional inputs are produced outside the system boundary (transplantation to harvesting), their inherent environmental burdens (such as fuel and energy consumed during manufacture and transportation) are transferred to the rice crop at the point of their use within the cultivation process indirectly (Fig. S2).

Life Cycle Assessment (LCA) Indicators

We quantified system footprints by summing outputs and activities and subtracting inputs, expressed through relevant LCA indicators such as carbon footprint, water footprint, global warming potential, and eutrophication potential (Fig. S2-S5). The general equation (Eq. 1) for calculating a system footprint across a defined study area is represented as:

$$\text{Footprint} = \sum(\text{Outputs} + \text{Activities}) \; - \sum(\text{Inputs}) \tag{1}$$

Carbon Footprint

Carbon Footprint (CF) is here assessed from the global warming potential (GWP) of each agricultural component over a 100-year period, expressed in kg C/ha (Eq. 2). This includes emissions from the production and application of synthetic fertilizers ($\text{CF}_{\text{Fertilizer}}$), the carbon embodied in pesticides used ($\text{CF}_{\text{Pesticides}}$), the carbon associated with seed production (CF_{Seeds}), fuel consumption from machinery operations ($\text{CF}_{\text{Machinery}}$), the energy used for irrigation pumping ($\text{CF}_{\text{Irrigation Pump}}$), GHG emissions resulting from the burning of rice residue in the field ($\text{CF}_{\text{Residue Burning}}$), and emissions of CH_4 and N_2O from the flooded paddy environment ($\text{CF}_{\text{CH}_4,\text{N}_2O}$). Details how each component was calculated and harmonized to 500 m resolution is available in Sections S1-S9.

$$\text{CF} = \text{CF}_{\text{Fertilizer}} + \text{CF}_{\text{Pesticides}} + \text{CF}_{\text{Seeds}} + \text{CF}_{\text{Machinery}} + \text{CF}_{\text{Irrigation Pump}} + \text{CF}_{\text{Residue Burning}} + \text{CF}_{\text{CH}_4,\text{N}_2O} \tag{2}$$

Nitrogen Footprint

Nitrogen Footprint (NF) in kg N/ha is calculated as Eutrophication Potential (EP) by modelling nutrient runoff, specifically nitrogen (N), which is derived from various N inputs. Key spatial inputs contributing to the EP calculation are derived from synthetic fertilizer (based on ICRISAT data), animal manure (Section S2), and crop residue returned (Section S3). This combined input is used for calculating from the average prediction from eight linear models (Table 1; Eq. 3).

$$NF = \frac{1}{8}\sum_{i=1}^{8}(m_i \times (\text{Fertilizer N} + \text{Manure N} + \text{Returned Residue N}) + c_i) \tag{3}$$

Here, m_i and c_i are the specific slope and intercept coefficients for each of the eight linear models.

Water Footprint

Water footprint is calculated by quantifying dynamic seasonal (S1 to S3) green and blue water consumption in rice cultivation using satellite-derived flood and vegetation indices (check Section S10 for details). For these dynamic rice seasons (S1 to S3), the seasonal Precipitation (P) from integrated multi-satellite retrievals for global precipitation measurement v7[76] and the seasonal Potential Evapotranspiration (PET) from MODIS were obtained. The Budyko method[77] was employed for Actual Evapotranspiration (AET) calculation. The AET is then calculated for each season using the Budyko empirical framework (Eq. 4), which relates AET to P and PET:

$$AET = P \times \sqrt{\left(\frac{PET}{P}\right)\tanh\left(\frac{P}{PET}\right)\left(1 - e^{-\frac{PET}{P}}\right)} \quad (4)$$

Using the calculated seasonal sums of Precipitation (P) and Budyko AET, the Green and Blue Water Footprints are then estimated. The Blue Water Footprint (WF_{blue}) represents the consumption of irrigation water, typically calculated as the water consumption (AET) that exceeds the available precipitation (Eq. 5). The Green Water Footprint (WF_{green}) represents the consumption of precipitation water. It is calculated as the actual evapotranspiration from this green water source that is utilized by crops (Eq. 6). The total water footprint is calculated as the sum of blue and green water footprints (Eq. 7). Based on the calculated P and AET, these can be estimated for each season:

$$WF_{\text{blue}} = \sum_{i=1}^{3} \max\left(0, AET_{S_i} - P_{S_i}\right) \quad (5)$$

$$WF_{\text{green}} = \sum_{i=1}^{3} \min\left(AET_{S_i}, P_{S_i}\right) \quad (6)$$

$$WF = WF_{\text{blue}} + WF_{\text{green}} \quad (7)$$

where, AET_{S_i} is the Actual Evapotranspiration in *mm* calculated for season i, and P_{S_i} is the Precipitation sum in *mm* for season i. The summation runs over the up to three rice growing seasons (i =1,2,3) identified within the year.

Rice Area and Yields

The methodology for mapping rice area and yield involved processing satellite imagery, climatic data, and management practice information, which included cloud masking, generating vegetation indices (NDVI, EVI, LSWI), and harmonizing all datasets to a 500 m resolution. Rice area was identified using a modified phenological algorithm that defines the growing season based on the interval between flooding events (≥ 80 days) and a maximum growing season EVI threshold (EVI > 0.4) to minimize misclassification. For yield estimation, a piece-wise linear regression (PLR) model was developed and trained on district-level data. To enhance model robustness and reduce overfitting, a novel metric, the Non-OVerfit Index (NOVI), was introduced. The model was optimized through a two-step process: first, tuning hyperparameters using a Randomized Iterative Convergence Evaluation (RICE) algorithm, and second, selecting the best-performing model structure from 10,000 iterations based on the highest NOVI score. A comprehensive description of the data processing, modeling, and validation procedures can be found in ref.[78].

Rice Sustainability Typologies

To systematically identify and differentiate rice cultivation areas exhibiting either sustainable or unsustainable cultivation practices, a spatially explicit Normalized Multi-Indexed Suitability (NMIS) raster was developed. This composite index was formulated by normalizing rice yield (RY') from -1 to 1 and 3 LCA indicators (carbon footprint (CF'), water footprint (WF') and nitrogen footprint (NF')) from 1 to -1 to obtain highly productive and low footprint regions and vice versa. To maintain spatio-temporal consistency, each LCA indicator normalized annually using their long term (2004-2021) minimum and maximum. Then, the NMIS raster is created by average these components (Eq. 8):

$$NMIS = \frac{RY' + CF' + NF' + WF'}{4} \quad (8)$$

Further, the NMIS raster was segregated based on its statistical quartiles (Q1 to Q4) (Table S4). The Q1 corresponds to regions practicing 'unsustainable' characterized by low rice yields and high associated environmental impacts. The Q2 is termed 'conventional' representing regions achieving reasonable yields accompanied by moderate environmental footprints. The Q3 denotes 'Productive' encompassing areas exhibiting moderate yields coupled with reasonable environmental impacts. Finally, the Q4 defines 'Sustainable' regions with high rice yields achieved with minimal environmental footprints. After these characterizations, the persistence of these typologies was identified by summing the annual typology raster's and dividing them by the study period.

Future rice typologies

To examine future changes, each rice typology was forecasted using annual percentage areas from 2004-2021. Initially, the annual time series data was pre-processed remove anomalous events by filtering 95% confidence interval outliers. For model development, the data was partitioned chronologically, with 2019–2021 for validation and 2004–2018 for training. Nine forecasting models were trained, including autoregressive integrated moving average (ARIMA), linear Regression, support vector regression, decision tree, random forest, extreme gradient boosting, neural network, long short-term memory, and transformers. A lagged feature engineering approach (n lags=3) was used for transforming the forecasting into a regression task to predict year 'y' using the inputs from years y−1 to y−3. Data was standardized for scaling-sensitive models, and hyperparameters (Table S5) were tuned via Optuna over 100 trials using the non-overfit index[78] as the objective function. Following optimization, 95% confidence intervals were generated to quantify uncertainty using model-specific methods, including residual bootstrapping, individual estimator variance, and quantile regression. The selected models under each typology are reported in supplementary Table S6.

Export Flows Analysis

To analyse the implications of rice cultivation typologies on global markets, the export data was acquired from the World Bank[19], which provides the quantity and monetary value of rice exported from India to each country (this dataset establishes the 'base case' scenario). To compute the environmental footprints transferred through exports, the analysis first established a footprint intensity for each impact category. For each typology (t) and the base case (b), the average annual rice yield (RY), carbon footprint (CF), nitrogen footprint (NF), and water footprint (WF) were calculated for the period 2004-2021. The footprint intensity ($I_{f,s}$) for a specific footprint (f) under a given scenario (s, where s is either a typology t or the base case b) was determined by dividing the average annual footprint by the average annual rice yield. This relationship is expressed by the equation (Eq. 9):

$$I_{f,s} = \frac{F_s}{RY_s} \quad (9)$$

where, F_s is the average annual footprint (i.e., CF_s, NF_s, or WF_s) and RY_s is the average annual rice yield for that scenario. The total exported footprint for a given typology ($F_{exp,t}$) (Eq. 10) was then calculated by multiplying the base case export quantity (Q_{exp}) by the corresponding footprint intensity of that typology ($I_{f,t}$).

$$F_{exp,t} = Q_{exp} \times I_{f,t} \quad (10)$$

For evaluating the economic implications, an eco-efficiency-adjusted revenue was computed. This began with calculating a Footprint Use Efficiency (FUE) metric for each typology and the base case. The FUE represents the amount of rice yield achieved per unit of environmental footprint, calculated as the inverse of footprint intensity (Eq. 11):

$$FUE_{f,s} = \frac{RY_s}{F_s} \quad (11)$$

A dimensionless conversion factor ($C_{f,t}$) was then derived for each typology relative to the base case by taking the ratio of their respective FUE values (Eq. 12):

$$C_{f,t} = \frac{FUE_{f,t}}{FUE_{f,b}} \quad (12)$$

This conversion factor quantifies the relative environmental efficiency of a typology compared to the current production mix (base case). A factor greater than one indicates that the typology is more efficient at generating yield for a given level of environmental impact. This factor was subsequently used to adjust the base case export revenue (R_b), obtained from the World Bank data, to estimate the adjusted revenue ($R_{adj,t}$) that would be generated if exports were sourced from that specific typology. The final adjusted revenue is given by (Eq. 13):

$$R_{adj,t} = R_b \times C_{f,t} \quad (13)$$

This calculation was performed separately for each environmental footprint, resulting in a carbon-adjusted, nitrogen-adjusted, and water-adjusted revenue for each of the four rice typologies, thereby linking economic value directly to environmental performance.

Acknowledgements

MN would like to thank the financial support through the CLIFF-GRADS Round 6 fellowship under the Global Research Alliance on Agricultural Greenhouse Gases (GRA) and the CGIAR Initiative on Low-Emission Food Systems (Mitigate+). This financial support provided essential personal and institutional resources for MN's research stay in University of Galway, Galway, Ireland. CS acknowledges financial support from (a) Research Ireland (formerly Science Foundation Ireland) for the Cytoheterosis Project (Grant Number: 19/FFP/6711 (RSF1676)), and from the (b) European Union Directorate General for International Partnerships (DG INTPA) funded for the LEG4DEV DESIRA project (https://leg4dev.org/; Grant Number: FOOD/2020/418-90).

Data Availability

All the data used in this study are publicly available or will be made available via Zenodo upon acceptance. These include the following datasets: MODIS burned areas[79], MODIS evapotranspiration[80], GPM precipitation[81], rice area and yield maps[78], ICRISAT district level agricultural statistics[56], ground water depths[62], rice exports data[19], and methane and nitrous oxide emissions from rice fields[10,11].

Code Availability

The analysis was performed using Python 3.11.2. The code will be made available via Zenodo upon acceptance.

References

1. Ahmad, A., Zoli, M., Latella, C. & Bacenetti, J. Rice cultivation and processing: Highlights from a life cycle thinking perspective. *Science of The Total Environment* **871**, 162079 (2023).
2. International Organization for Standardization (ISO). Environmental Management: Life Cycle Assessment - Principles and Framework. (2020).
3. Harris, S. & Narayanaswamy, V. *A Literature Review of Life Cycle Assessment in Agriculture*. (RIRDC, 2009).
4. Marques, C., Güneş, S., Vilela, A. & Gomes, R. Life-Cycle Assessment in Agri-Food Systems and the Wine Industry—A Circular Economy Perspective. *Foods* **14**, 1553 (2025).
5. Taylor, I. *et al.* Nature-positive goals for an organization's food consumption. *Nat Food* **4**, 96–108 (2023).
6. Jwaideh, M. A. A. & Dalin, C. The multi-dimensional environmental impact of global crop commodities. *Nat Sustain* **8**, 396–410 (2025).
7. Singh, G., Gupta, M. K., Chaurasiya, S., Sharma, V. S. & Pimenov, D. Y. Rice straw burning: a review on its global prevalence and the sustainable alternatives for its effective mitigation. *Environ Sci Pollut Res* **28**, 32125–32155 (2021).
8. Singh, P., Singh, G., Sodhi, G. P. S. & Benbi, D. K. Accounting Carbon Footprints and Applying Data Envelopment Analysis to Optimize Input-Induced Greenhouse Gas Emissions Under Rice–Wheat Cropping System in North-Western India. *J Soil Sci Plant Nutr* **21**, 3030–3050 (2021).
9. Ministry of Agriculture and Farmers Welfare, Department of Agriculure and Farmers Welfare. *Annual Report 2023-24*. 360 https://agriwelfare.gov.in/Documents/AR_English_2023_24.pdf (2024).
10. Sahil, F. M., Narayanan, M. & Ilampooranan, I. Nitrous oxide emissions dynamics in Indian agricultural landscapes: Revised emission rates and new insights. *Agriculture, Ecosystems & Environment* **356**, 108639 (2023).
11. Sahil, F. M., Narayanan, M. & Ilampooranan, I. Setting Up Methane Mitigation Measures for Indian Rice Fields: Representative Emissions and New Interpretations. *Global Biogeochemical Cycles* **38**, e2024GB008107 (2024).
12. Bhattacharyya, R. *et al.* Soil degradation and mitigation in agricultural lands in the Indian Anthropocene. *European J Soil Science* **74**, e13388 (2023).
13. Karnataka Regional Office. *State Focus Paper, Karnataka, 2024-2025*. (2024).
14. Taylor, M. & Bhasme, S. Why Do Farmers Disadopt Successful Innovations? Socio-Ecological Niches and Rice Intensification. *Agronomy* **14**, 2238 (2024).
15. Ramana, M. V. *et al.* Integrated Farming Systems Improve the Income of Small Farm Holdings—An Overview of Earlier Findings in the Indian Context. *Food and Energy Security* **14**, e70064 (2025).
16. Coggins, S. *et al.* Data-driven strategies to improve nitrogen use efficiency of rice farming in South Asia. *Nat Sustain* **8**, 22–33 (2025).
17. Burney, J. & Ramanathan, V. Recent climate and air pollution impacts on Indian agriculture. *Proc. Natl. Acad. Sci. U.S.A.* **111**, 16319–16324 (2014).
18. Maiti, A. *et al.* Optimal rainfall threshold for monsoon rice production in India varies across space and time. *Commun Earth Environ* **5**, 302 (2024).
19. World Bank WITS. India Rice Exports by Country, 2023. (2023).
20. Glauber, J. W. & Mamun, A. *Global Rice Market: Current Outlook and Future Prospects*. https://hdl.handle.net/10568/168523 (2024).
21. MINISTRY OF STATISTICS AND PROGRAMME IMPLEMENTATION. *STATE-WISE AND ITEM-WISE VALUE OF OUTPUT FROM AGRICULTURE, FORESTRY AND FISHING*. (2023).
22. Zhang, G. *et al.* Fingerprint of rice paddies in spatial–temporal dynamics of atmospheric methane concentration in monsoon Asia. *Nat Commun* **11**, 554 (2020).
23. Zhang, B. *et al.* Methane emissions from global rice fields: Magnitude, spatiotemporal patterns, and environmental controls. *Global Biogeochemical Cycles* **30**, 1246–1263 (2016).
24. Qian, H. *et al.* Greenhouse gas emissions and mitigation in rice agriculture. *Nat Rev Earth Environ* **4**, 716–732 (2023).
25. Cassman, K. G. & Grassini, P. A global perspective on sustainable intensification research. *Nat Sustain* **3**, 262–268 (2020).
26. Yuan, S. *et al.* Sustainable intensification for a larger global rice bowl. *Nat Commun* **12**, 7163 (2021).
27. Jahangir, M. M. R. *et al.* Carbon footprint and greenhouse gas emissions of different rice-based cropping systems using LCA. *Sci Rep* **15**, 10214 (2025).

28. Paramesh, V. *et al.* A Life Cycle Assessment of Rice–Rice and Rice–Cowpea Cropping Systems in the West Coast of India. *Land* **12**, 502 (2023).
29. Abdul Rahman, M. H. *et al.* Life cycle assessment in conventional rice farming system: Estimation of greenhouse gas emissions using cradle-to-gate approach. *Journal of Cleaner Production* **212**, 1526–1535 (2019).
30. Poore, J. & Nemecek, T. Reducing food's environmental impacts through producers and consumers. *Science* **360**, 987–992 (2018).
31. Gupta, R. & Mishra, A. Climate change induced impact and uncertainty of rice yield of agro-ecological zones of India. *Agricultural Systems* **173**, 1–11 (2019).
32. Intergovernmental Panel on Climate Change (IPCC). Chapter 5: Croplands. in *2006 IPCC Guidelines for National Greenhouse Gas Inventories* 1–54 (IPCC, 2006).
33. Manjunath, K. R., More, R. S., Jain, N. K., Panigrahy, S. & Parihar, J. S. Mapping of rice-cropping pattern and cultural type using remote-sensing and ancillary data: a case study for South and Southeast Asian countries. *International Journal of Remote Sensing* **36**, 6008–6030 (2015).
34. Ajay, A. *et al.* Large survey dataset of rice production practices applied by farmers on their largest farm plot during 2018 in India. *Data in Brief* **45**, 108625 (2022).
35. Nayak, H. S. *et al.* Context-dependent agricultural intensification pathways to increase rice production in India. *Nat Commun* **15**, 8403 (2024).
36. Gumma, M. K., Nelson, A., Thenkabail, P. S. & Singh, A. N. Mapping rice areas of South Asia using MODIS multitemporal data. *Journal of Applied Remote Sensing* **5**, 053547–053547 (2011).
37. Narayanan, M. & Ilampooranan, I. Mapping Indian Rice Yields Through Statistical Modeling Using Satellite and Climatic Data. in *IEEE International Geoscience and Remote Sensing Symposium* (2023).
38. Frankenberg, C. *et al.* Global column-averaged methane mixing ratios from 2003 to 2009 as derived from SCIAMACHY: Trends and variability. *Journal of Geophysical Research* **116**, D04302 (2011).
39. Parker, R. *et al.* Methane observations from the Greenhouse Gases Observing SATellite: Comparison to ground-based TCCON data and model calculations. *Geophysical Research Letters* **38**, (2011).
40. Hasekamp, O. *et al. Algorithm Theoretical Baseline Document for Sentinel-5 Precursor Methane Retrieval*. https://sentinels.copernicus.eu/documents/247904/2476257/Sentinel-5P-TROPOMI-ATBD-Methane-retrieval.pdf/f275eb1d-89a8-464f-b5b8-c7156cda874e?t=1658313508597 (2022).
41. Azzari, G. *et al.* Satellite mapping of tillage practices in the North Central US region from 2005 to 2016. *Remote Sensing of Environment* **221**, 417–429 (2019).
42. Brinkhoff, J., Dunn, B. W. & Robson, A. J. Rice nitrogen status detection using commercial-scale imagery. *International Journal of Applied Earth Observation and Geoinformation* **105**, 102627 (2021).
43. Chatterjee, S., Debnath, S. & Yumnam, N. The role of farm subsidies in changing India's water footprint. *Nature Communications* **15**, 8742 (2024).
44. Debnath, S., Chatterjee, S. & Bora, A. Assessment of rice yield gap under a changing climate in India. *Journal of Water and Climate Change* **12**, 1245–1264 (2021).
45. Yumnam, N., Debnath, S. & Bora, A. Critical weather limits for paddy rice under diverse ecosystems of India. *Frontiers in Plant Science* **14**, 1226064 (2023).
46. Pradhan, S. K., Nayak, A. K. & Mohanty, M. *Advances in Rice Breeding: Stress Tolerance, Climate Resilience, Quality, and High Yield*. (ICAR-National Rice Research Institute, 2021).
47. Verma, R. *et al. Hybrid Rice Seed Production Technology*. 44 https://icar-nrri.in/wp-content/uploads/2021/08/Research-Bulletin-No-31-Hybrid-Rice-Seed-Production-Technology.pdf (2021).
48. Press Information Bureau. *Empowering India's Farmers Through Strategic Fertilizer Policy*. https://www.pib.gov.in/PressNoteDetails.aspx?NoteId=154966&ModuleId=3 (2025).
49. Bhatia, A., Jain, N. & Pathak, H. Methane and nitrous oxide emissions from Indian rice paddies, agricultural soils, and crop residue burning. *Greenhouse Gases: Science and Technology* **3**, 356–371 (2013).
50. Samal, P., Behura, D., Prusty, B. K. & Mishra, S. N. Efficiency and sustainability in rice production across Indian states. *Environmental Research: Food Systems* **2**, 025008 (2025).
51. Kritee, K., Malla, S. & Davidson, E. A. High nitrous oxide fluxes from rice indicate the need to manage water for both long- and short-term climate impacts. *Proceedings of the National Academy of Sciences* **115**, 9720–9725 (2018).
52. Shyamsundar, P. *et al.* Fields on fire: Alternatives to crop residue burning in India. *Science* **365**, 536–538 (2019).

53. Van Soest, P. J. Rice straw, the role of silica and treatments to improve quality. *Animal Feed Science and Technology* **130**, 137–171 (2006).
54. Duncan, A. J., Samaddar, A. & Blümmel, M. Rice and wheat straw fodder trading in India: Possible lessons for rice and wheat improvement. *Field Crops Research* **246**, 107680 (2020).
55. Wang, Y. *et al.* Toughening effect and mechanism of rice straw Fiber-reinforced lime soil. *Construction and Building Materials* **393**, 132133 (2023).
56. ICRISAT. International Crops Research Institute for the Semi-Arid Tropics (ICRISAT)-District Level Data. (2017).
57. Praveen, K. *et al.* Indian fertilizer subsidy conundrum: Tracking the recent developments. *Indian J Agri Sci* **91**, 608–612 (2021).
58. Gawdiya, S. *et al.* Field-Based Evaluation of Rice Genotypes for Enhanced Growth, Yield Attributes, Yield and Grain Yield Efficiency Index in Irrigated Lowlands of the Indo-Gangetic Plains. *Sustainability* **15**, 8793 (2023).
59. Jaldhani, V. *et al.* Rice biofortification in India: Progress, adoption, and potential. *Tropical Agriculture* **102**, (2025).
60. Sinha, E., Michalak, A. M., Balaji, V. & Resplandy, L. India's Riverine Nitrogen Runoff Strongly Impacted by Monsoon Variability. *Environ. Sci. Technol.* **56**, 11335–11342 (2022).
61. Likun, A. *et al.* Water Footprint Analysis of Wheat Cultivation in the Ganga Yamuna Doab Region – Implications for Sustainable Water Management. *Environmental Challenges* **19**, 101162 (2025).
62. Verkaik, J., Sutanudjaja, E. H., Oude Essink, G. H. P., Lin, H. X. & Bierkens, M. F. P. GLOBGM v1.0: a parallel implementation of a 30\,arcsec PCR-GLOBWB-MODFLOW global-scale groundwater model. *Geoscientific Model Development* **17**, 275–300 (2024).
63. Kayatz, B. *et al.* "More crop per drop": Exploring India's cereal water use since 2005. *Science of The Total Environment* **673**, 207–217 (2019).
64. Negi, D. S., Birthal, P. S., Roy, D. & Khan, M. T. *Adoption and Impact of Hybrid Rice in India*. https://cgspace.cgiar.org/handle/10568/110121 (2020).
65. Kumar, N. *et al.* Challenges and opportunities in productivity and sustainability of rice cultivation system: a critical review in Indian perspective. *CEREAL RESEARCH COMMUNICATIONS* **50**, 573–601 (2022).
66. Nayak, H. S. *et al.* Pathways and determinants of sustainable energy use for rice farms in India. *Energy* **272**, 126986 (2023).
67. Ministry of Agriculture & Farmers Welfare. National Mission for Sustainable Agriculture (NMSA). (2018).
68. Deep, M., Kumar, R. M., Saha, S. & Singh, A. Rice-based cropping systems for enhancing productivity of food grains in India: decadal experience of AICRP. *Indian Farming* **68**, 27–30 (2018).
69. Surendhar, M., Anbuselvam, Y. & Ivin, J. J. S. Status of rice cultivation under Indian saline lowlands. *J Pharmacogn Phytochem* **10**, 371–376 (2021).
70. Ministry of Agriculture & Farmers Welfare. Union Agriculture Minister Shri Shivraj Singh Chouhan Announces Two Genome-Edited Rice Varieties Developed in India. (2025).
71. Anantha, M. S. *et al.* Trait Combinations That Improve Rice Yield under Drought: Sahbhagi Dhan and New Drought-Tolerant Varieties in South Asia. *Crop Science* **56**, 408–421 (2016).
72. Anumalla, M. *et al.* Future flooding tolerant rice germplasm: Resilience afforded beyond *Sub1A* gene. *The Plant Genome* **18**, e70040 (2025).
73. Beyer, R. M., Hua, F., Martin, P. A., Manica, A. & Rademacher, T. Relocating croplands could drastically reduce the environmental impacts of global food production. *Communications Earth & Environment* **3**, 49 (2022).
74. World Bank. World Development Indicators. (2026).
75. Deekshithulu, N. G., Kanth, B. K., Tejaswini, V., Tejaswini, V. & Thomson, T. Trends and patterns of farm mechanization in India. *Int. J. Adv. Biochem. Res.* **8**, 843–856 (2024).
76. Huffman, G. J. *et al.* Integrated multi-satellite retrievals for the global precipitation measurement (GPM) mission (IMERG). in *Satellite precipitation measurement: Volume 1* 343–353 (Springer, 2020).
77. Budyko, M. I. *Climate and Life*. (Academic Press, Orlando, FL, 1974).
78. Narayanan, M., Sharma, A. & Ilampooranan, I. Spatio-temporally Explicit Decoupling of Rice Yield and Methane Emission Relationships in India. *SSRN Electronic Journal* https://dx.doi.org/10.2139/ssrn.5781084 (2025) doi:https://dx.doi.org/10.2139/ssrn.5781084.
79. Giglio, L., Boschetti, L., Roy, D. P., Humber, M. L. & Justice, C. O. The Collection 6 MODIS burned area mapping algorithm and product. *Remote Sensing of Environment* **217**, 72–85 (2018).

80. Mu, Q., Heinsch, F. A., Zhao, M. & Running, S. W. Development of a global evapotranspiration algorithm based on MODIS and global meteorology data. *Remote Sensing of Environment* **111**, 519–536 (2007).
81. Precipitation Processing System (PPS) At NASA GSFC. GPM IMERG Final Precipitation L3 1 month 0.1 degree x 0.1 degree V06. NASA Goddard Earth Sciences Data and Information Services Center https://doi.org/10.5067/GPM/IMERG/3B-MONTH/06 (2022).
82. Howarth, R. W. An assessment of human influences on fluxes of nitrogen from the terrestrial landscape to the estuaries and continental shelves of the North Atlantic Ocean. *Nutrient Cycling in Agroecosystems* **52**, 213–223 (1998).
83. Boyer, E. W., Goodale, C. L., Jaworski, N. A. & Howarth, R. W. Anthropogenic nitrogen sources and relationships to riverine nitrogen export in the northeastern U.S.A. *Biogeochemistry* **57**, 137–169 (2002).
84. Chen, F. *et al.* Net anthropogenic nitrogen inputs (NANI) into the Yangtze River basin and the relationship with riverine nitrogen export. *JGR Biogeosciences* **121**, 451–465 (2016).
85. Hong, B. *et al.* Advances in NANI and NAPI accounting for the Baltic drainage basin: spatial and temporal trends and relationships to watershed TN and TP fluxes. *Biogeochemistry* **133**, 245–261 (2017).
86. Hong, B., Swaney, D. P. & Howarth, R. W. Estimating Net Anthropogenic Nitrogen Inputs to U.S. Watersheds: Comparison of Methodologies. *Environ. Sci. Technol.* **47**, 5199–5207 (2013).
87. Hong, B. *et al.* Evaluating regional variation of net anthropogenic nitrogen and phosphorus inputs (NANI/NAPI), major drivers, nutrient retention pattern and management implications in the multinational areas of Baltic Sea basin. *Ecological Modelling* **227**, 117–135 (2012).
88. Howarth, R. W. *et al.* The influence of climate on average nitrogen export from large watersheds in the Northeastern United States. *Biogeochemistry* **79**, 163–186 (2006).
89. Goyette, J., Bennett, E. M., Howarth, R. W. & Maranger, R. Changes in anthropogenic nitrogen and phosphorus inputs to the St. Lawrence sub-basin over 110 years and impacts on riverine export. *Global Biogeochemical Cycles* **30**, 1000–1014 (2016).

Figures

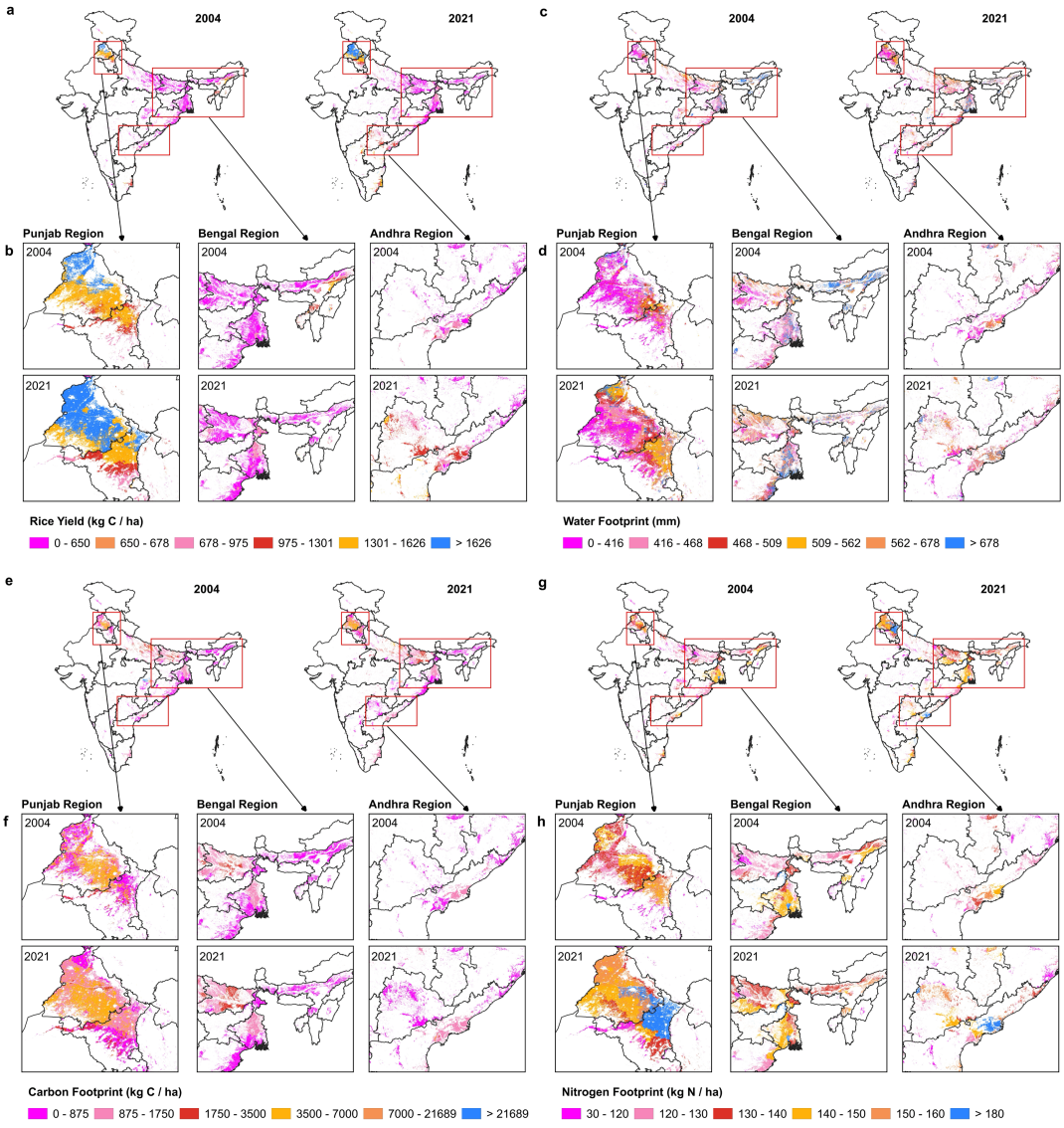

Figure 1: Fine-scale mapping of spatio-temporal variations of Life Cycle Assessment (LCA) indicators for rice cultivation across India between 2004 and 2021. The figure displays maps for (a, b) rice yield (kg C/ha), (c, d) water footprint (mm), (e, f) carbon footprint (kg C/ha), and (g, h) nitrogen footprint (kg N/ha). Panels (a, c, e, g) provide a pan-India overview, while panels (b, d, f, h) offer detailed views of three major rice-growing regions: Punjab, Bengal, and Andhra.

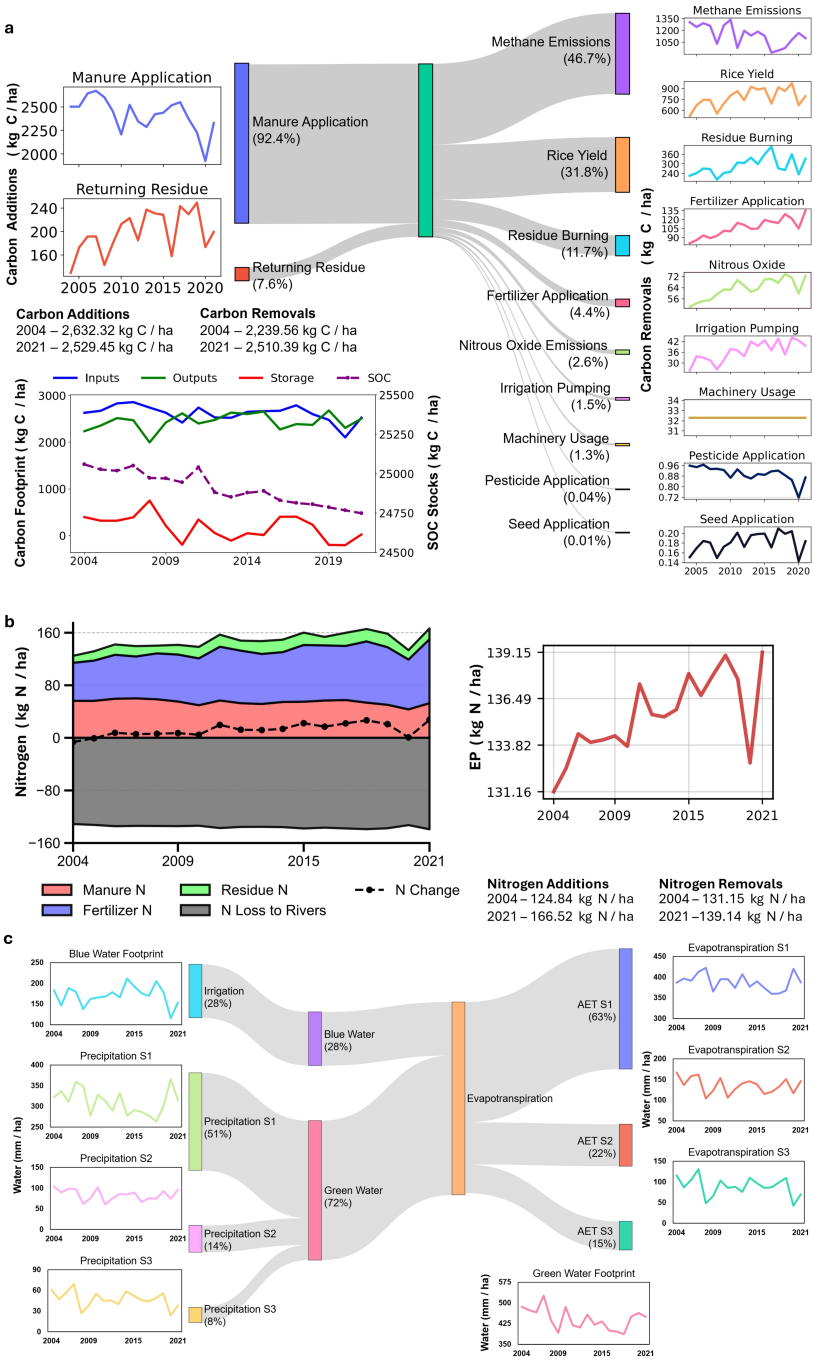

Figure 2: Temporal dynamics and budgets of carbon, nitrogen, and water footprints in the rice cultivation agroecosystem in India from 2004 to 2021. (a) The carbon cycle, illustrated with a Sankey diagram showing the relative contribution of different fluxes to total carbon additions and removals. Time-series plots detail the annual trends of major inputs (Manure Application and Returning Residue), outputs (e.g., Methane Emissions, Rice Yield, etc.), and the overall budget, including the Carbon Footprint (Inputs), Carbon Removals (Outputs), and resulting Soil Organic Carbon (SOC) Stocks. (b) The nitrogen budget, depicted as a stacked area chart showing annual inputs (Manure N, Fertilizer N), outputs (Residue N, N Loss to Rivers), and the net annual change in system nitrogen (N Change). An accompanying time-series plot shows the trend of the Eutrophication Potential (EP). (c) The water budget, visualized with a Sankey diagram partitioning water inputs into Blue Water (irrigation) and Green Water (precipitation) and tracking their flow to various Actual Evapotranspiration (AET) outputs. Associated time-series plots show the annual and seasonal trends for the Blue and Green Water Footprints and their constituent components.

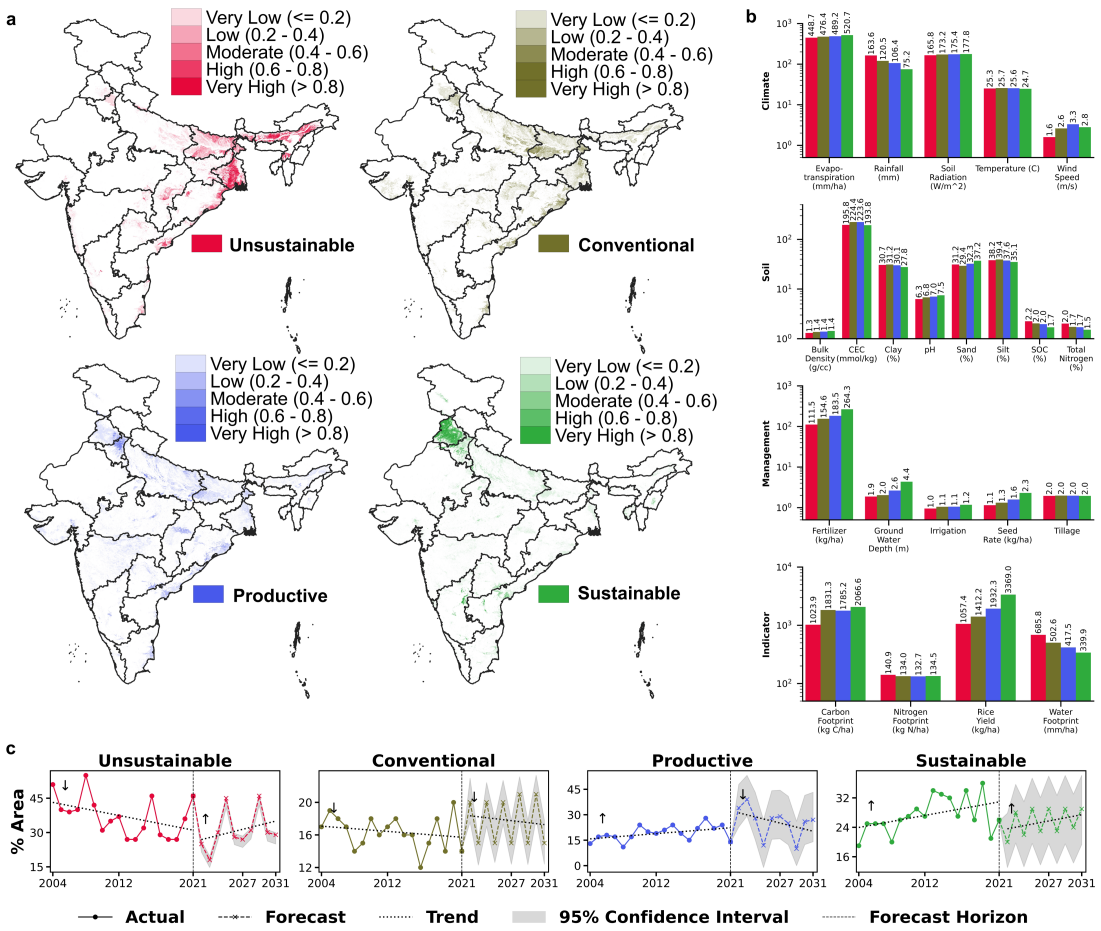

Figure 3: Spatial and temporal analysis of rice cultivation typologies across India. (a) Annual persistence heat maps illustrating the geographical distribution and temporal fluctuations of four distinct rice cultivation typologies: Unsustainable, Conventional, Productive, and Sustainable. The maps depict the prevalence of each typology across different regions of India over the period from 2004 to 2021. Note: Individual heat maps of typologies across years 2004,2009, 2014 and 2021 are shown in Fig. S1 to illustrate fluctuations in typologies. The scale bar represents the persistence of cultivation. (b) Bar charts showing the characteristic mean values for various environmental and agricultural parameters associated with each of the four cultivation typologies. The parameters are organized into four groups: Climate (Evapo-transpiration in mm/ha, Rainfall in mm/ha, Soil Radiation in W/m², Temperature in °C, and Wind in m/s), Soil (Bulk Density in g/cc, Cation Exchange Capacity (CEC) in mmol/kg, Clay in %, pH, Sand in %, Silt in %, Soil Organic Carbon (SOC) in %, and Total Nitrogen in %), Management (Fertilizer in kg/ha, Groundwater Depth in m, Irrigation (with values ranging from 0 to 2; with high values indicating higher irrigation intensity), Seed Rate in kg/ha, and Tillage in %), and Indicator variables (Carbon Footprint in kg C/ha, Nitrogen Footprint in kg N/ha, Rice Yield in kg/ha, and Water Footprint in mm/ha). (c) Time series plots and forecasts for the percentage area of each cultivation typology. The plots show the actual data from 2004 to 2021 (solid line), the long-term trend (dashed line), the 95% confidence interval (shaded grey area), and the forecast extending to 2031 (dotted line). Black arrows indicate visually distinct peaks or troughs in the time series.

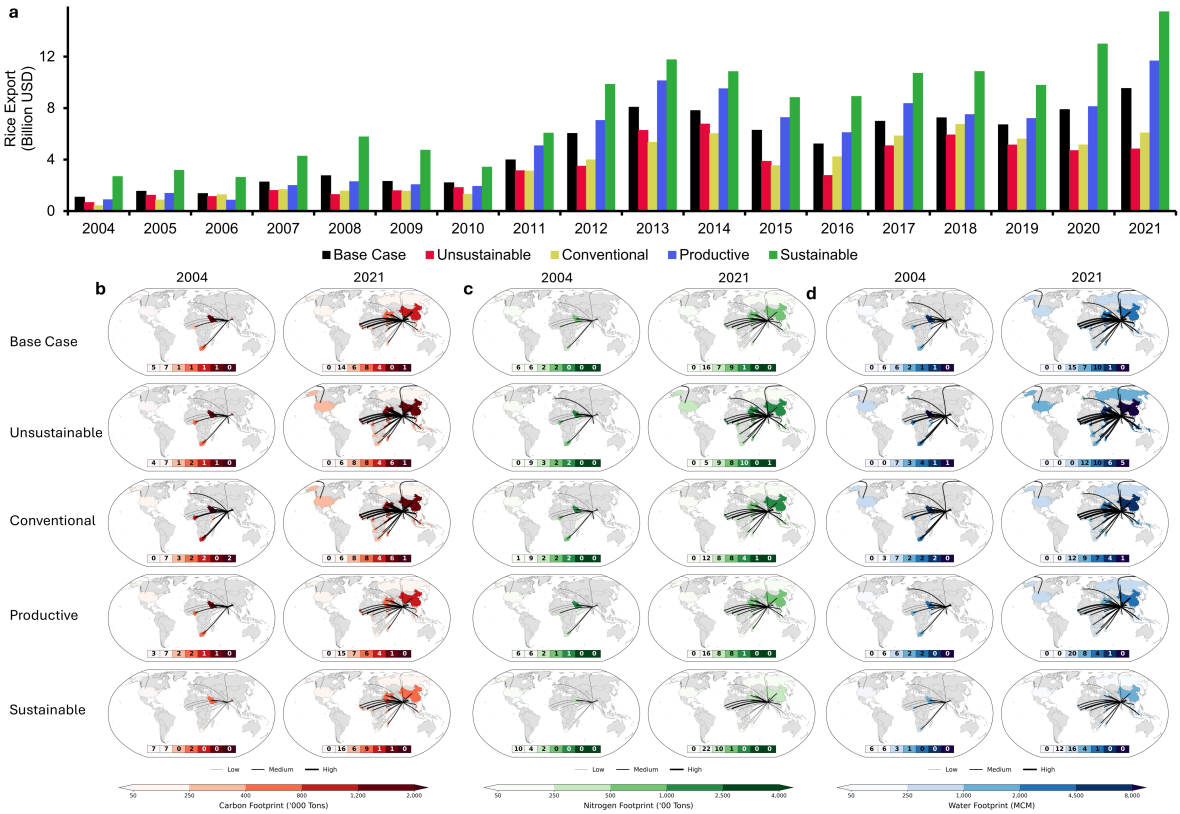

744

745 **Figure 4:** Geographical distribution and magnitude of environmental footprints associated with India's
746 rice exports for the years 2004 and 2021 across five distinct agricultural production scenarios: Base
747 case, Unsustainable, Conventional, Productive, and Sustainable. The figure is organized into four main
748 panels: (a) Trade value of exports in US dollars, (b) Carbon Footprint (CF) in thousand tonnes of carbon,
749 (c) Nitrogen Footprint (NF) in thousand tonnes of nitrogen, and (d) Water Footprint (WF) in million cubic
750 meters (MCM). Each map visualizes the footprint for importing nations (Top 90%) using a choropleth
751 color scale, where darker shades indicate a higher environmental impact. Black lines represent the
752 export flows from India to its trade partners, with line thickness corresponding to the magnitude of the
753 footprint (Low, Medium, High). Below each map, a segmented bar chart quantifies the number of trade
754 partner countries falling into each distinct footprint category, with color matching the map's legend.

Tables

Table 1: Functional units used in the LCA

Component Category	Component Name	Functional Unit
LCA Indicators	Carbon Footprint (CF)	*kg C/ha*
	Water Footprint (WF)	*mm/ha*
	Nitrogen Footprint (NF)	*kg N/ha*
Agricultural Outputs	Rice Yield	*kg C/ha*
	Rice Area	*ha*
	Above-ground Biomass	*kg C/ha*
	Below-ground Biomass	*kg C/ha*
Material & Energy Inputs	Synthetic Fertilizer Application (N, P, K)	*kg C/ha*
	Animal Manure Application	*kg C/ha*
	Rice Residue Returned	*kg C/ha*
	Pesticide Application Rate	*kg C/ha*
	Seeding Rate	*kg C/ha*
	Machinery (Land Preparation and Threshing)	*kg C/ha*
	Irrigation Pumping Energy	*kg C/ha*
Direct Emissions	Rice Residue Burning	*kg C/ha*
	Methane (CH_4) from Rice	*kg C/ha*
	Nitrous Oxide (N_2O) from rice fields	*kg C/ha*
Integrated Assessment	Normalized Multi-Indexed Suitability	*No Units*

Table 2: Empirical linear models (Y=mx+c) utilized to calculate components of the riverine nutrient flux for the Eutrophication Potential assessment. The independent variable 'x' corresponds to the calculated combined nitrogen input, while the dependent variable 'Y' represents the predicted nutrient flux component. The coefficient of determination (R^2) for each model and its source are also provided.

S. No.	Coefficients	Source
1.	m = 0.2; c = 102.5 R^2 = 0.73	Ref. [82]
2.	m = 0.25; c = 7.2 R^2 = 0.62	Ref. [83]
3.	m = 0.164; c = 74.887 R^2 = 0.59	Ref. [84]
4.	m = 0.17; c = 142 R^2 = 0.92	Ref. [85]
5.	m = 0.21; c = 117.76 R^2 = 0.24	Ref. [86]
6.	m = 0.13; c = 201.4 R^2 = 0.92	Ref. [87]
7.	m = 0.26; c = 107 R^2 = 0.62	Ref. [88]
8.	m = 0.15; c = 105 R^2 = 0.87	Ref. [89]

Supplementary: Water-efficient Indian rice cultivation boosts exports despite high carbon footprints

Mukund Narayanan[a,b], Idhayachandhiran Ilampooranan[a]*, Peter C. McKeown[b], Ankit Sharma[a], Noel Ndlovu[b], & Charles Spillane[b]*

[a]*Department of Water Resources Development and Management, Indian Institute of Technology Roorkee, Roorkee, Uttarakhand, India*
[b]*Agricultural Systems and Bio-economy Group, University of Galway, Galway, Ireland*
**Corresponding Authors:*
Idhayachandhiran Ilampooranan – idhaya@wr.iitr.ac.in
Charles Spillane – charles.spillane@universityofgalway.ie

ORCID:

Mukund Narayanan (MN) – 0000-0001-9558-320X
Idhayachandhiran Ilampooranan (II) – 0000-0003-0819-376X
Peter C. McKeown (PM) – 0000-0002-7255-6062
Ankit Sharma (AS) – 0009-0007-4294-0753
Noel Ndlovu (NN) – 0000-0002-1832-0251
Charles Spillane (CS) – 0000-0003-0819-376X

Sections S1 to S13
Figures S1 to S4
Tables S1 to S7

Section S1 - Synthetic Fertilizer

District-level synthetic fertilizer consumption data for Nitrogen (N), Phosphorous (P), and Potassium (K) was obtained from the International Crops Research Institute for the Semi-Arid Tropics (ICRISAT)[1]. Although fine-scale, farm-level data is preferred for LCA, district-level data was the highest available spatial resolution across India for synthetic fertilizer production and served as the basis for this assessment. To spatially disaggregate this district-level fertilizer data to a 500 *m* resolution (aligning it with satellite product resolution) and masking it to identified rice cultivation areas, an apportionment method was developed (refer to Section S11 for details). For calculating the carbon footprint associated with apportioned fertilizer use, carbon footprint factors based on Lal (2004) were applied. The factors used for nitrogen, phosphates and potassium fertilizers were CF_N = 1.3 *kg C / kg N*, CF_{P} = 0.20 *kg C kg* P_2O_5, and CF_K = 0.15 *kg C kg* K_2O, respectively. The total carbon footprint from fertilizer application for a given area can be calculated using the following equation (Eq. 8):

$$\mathrm{CF_{Fertilizer}} = (\mathrm{Rate_N} \times \mathrm{CF_N}) + (\mathrm{Rate_P} \times \mathrm{CF_P}) + (\mathrm{Rate_K} \times \mathrm{CF_K}) \quad (8)$$

where, $CF_{Fertilizer}$ is the carbon footprint from fertilizer application (*kg C/ha*), $Rate_N$, $Rate_P$, and $Rate_K$ are the application rates of N, P, and K fertilizers respectively (*kg/ha*).

Section S2 - Animal Manure

District-level animal manure data was acquired from Sahil et al.[2]. Following the same methodology applied to synthetic fertilizers, this data was apportioned to rice cultivation areas within each district. Estimates of animal manure on rice were derived by calculating district rice area proportion, applying it to total manure, and converting this to a kg/ha rate. This rate was mapped to create a 500 m gridded dataset of estimated application rates across India. The carbon footprint from animal manure is estimated by multiplying the manure application rate by a conversion factor to carbon equivalent (Eq. 9).

$$\mathrm{CF_{Manure}} = AR_{Manure} \times 0.37 \quad (9)$$

Where AR_{Manure} is the estimated animal manure application rate in kg/ha, and 0.37 is the factor used to convert this rate to kg C/ha obtained from ref. [3].

Section S3 - Rice Residue Return

To quantify biomass contributions, unburned rice pixels were isolated by masking MODIS fire data (MCD64A1.061) from rice areas[4]. Total biomass was calculated using yield data and the harvest index before estimating below-ground biomass via root-to-shoot ratios (Section S12). We applied residue return factors for above-ground (5%) and below-ground roots (100%) to determine the total residue returned[5]. The final residue amounts were converted to carbon equivalents using the standard calculation method (Eq. 10) provided below:

$$\mathrm{CF_{Residue\ Return}} = \left((B_{\mathrm{above}} \times 0.05) + (B_{\mathrm{below}})\right) \times C_{\mathrm{fraction}} \quad (10)$$

Where B_{above} and B_{below} are the estimated above-ground and below-ground biomass in kg/ha, respectively, and C_{fraction} is the carbon content fraction used to convert biomass to carbon mass. The resulting contribution is expressed in kg C/ha.

Section S4 - Pesticide Application

To predict pesticide usage without fine-scale data, for scale independence, a polynomial linear model (R^2 = 0.8; Table S4) utilized national yield and fertilizer intensities (kg/ha values) from 2004 to 2021. We applied this validated model to generate fine-resolution predictions at 500 *m*, assuming consistent relationships between agricultural inputs and crop productivity. To estimate carbon footprint, the predicted pesticide quantities were converted using a standard carbon cost factor (4.93 *kg* C / *kg*) for calculation. Refer to Section S13 and Table S4 for further details.

Section S5 - Seeding

Like pesticide data, obtaining detailed data on the quantity of seed applied at the pixel scale presents challenges. Consequently, an approach was developed to predict seed application rates at

the pixel scale using correlations derived from data available at the national level. A linear model (R^2 = 0.3; Table S4) using historical data from 2004-2021 was constructed specifically to analyze the relationship between seed application rates and rice yield using national aggregate data. National-level model was used to predict seed application at 500 *m* resolution based on pixel-level rice yield estimates; all datasets were normalized to kg/ha to maintain scale independence. Further, Carbon footprint for seeding was calculated based on detailed energy budgets for each crop's seed production process, excluding packaging emissions. The average carbon footprint factors of 0.257 kg C / kg seed from ref. [6] was multiplied with the seeding rate to obtain the carbon footprint.

Section S6 - Machinery Usage for Land Preparation, Threshing, and Harvesting

No data is available for tractor usage across India, so we estimated this based on assumptions derived from ref.[7]. These assume (a) Seed-bed preparation, involving one disking, two cultivator passes, and one pulverization, has a carbon footprint of 25.2 kg C/ha, and (b) the combined processes of seeding, harvesting, and threshing account for a carbon usage of 7.1 kg C/ha.

Section S7 - Irrigation Pumping Fuel and Electricity

This calculation estimates the carbon footprint (kg C/ha) from irrigation pumping for rice cultivation by utilizing annual datasets for groundwater depth[8] and rice yield[4]. The physics of lifting water is described by the work-energy relationship. Theoretically, lifting 1000 cubic m of water by 1 m requires 2.724 *kWh*. However, assuming 30% pump efficiency, the effective energy required is ~9.08 kWh[9]. This estimation is using the following equation (Eq. 10):

$$\mathrm{CF}_{\text{Irrigation Pump}} = \frac{\mathrm{RY} \times 2.5 \times 9.08 \times 1.3 \times GW_{\text{depth}}}{1000} \times \left(\frac{11745137 \times EF_{\text{electric}} + 21736459 \times EF_{\text{diesel}}}{33481596} \right) \quad (11)$$

Here, RY is the annual rice yield, and GW_{depth} is the annual mean ground water depth. The constant 2.5 m^3 is linked to yield-to-water requirement conversion based on ref.[10] and ref.[11]. The factor 1.3 is applied to account for transmission losses during pumping based on ref.[7]. The division by 1000 performs a unit conversion. The final term is a weighted average emission factor, combining emission factors for electric (EF_{electric}) and diesel (EF_{diesel}) pumping from ref.[7]. The weights (11745137 for electric, 21736459 for diesel) and the total divisor (33481596) reflect a total number of electric and diesel pumps on the national scale[12].

Section S8 - Rice Residue burning

Burned areas were segregated from unburned areas using MODIS burned area maps and then intersected with rice yield maps[4]. Within the areas identified as burned, the amount of above-ground rice residue (A_f) that contributed to the burning event was quantified through estimating the total residue produced.

Since not all residue is fully combusted, the amount of burned residue is then calculated, considering a burnt fraction (B_f), a dry matter fraction (D_f) and a fraction oxidized (C_f) to represent the combustible portion. This quantity was then used for estimating greenhouse gas emissions, such as CO_2, CH_4, and N_2O, following IPCC[13]. The general equation (Eq. 12) used to calculate emissions from crop residue burning ($CF_{Residue\ Burning}$) is:

$$CF_{Residue\ Burning} = \mathrm{A}_f \times B_f \times C_f \times D_f \times E_{\mathrm{b}} \quad (12)$$

where, the B_f value is 0.89[14], the C_f value is 0.8[14], the D_f value is 0.86[15], and E_b is the emission factor for a specific greenhouse gas: 1.46 kg CO_2/kg[16], 0.027 kg CH_4/kg[17], and 0.00007 kg N_2O/kg[17]. These emissions of non-CO_2 gases like CH_4 and N_2O are converted to CO_2-equivalents using 28 for CH_4 and 295 for N_2O over a 100-year period[13]. The total CO_2 equivalent mass is then converted to carbon mass by multiplying by the ratio of the molecular weight of carbon to CO_2 (12/44) to get the carbon footprint in C equivalents.

Section S9 - CH_4 and N_2O Emissions

Methane (CH_4) production in rice area is primarily an anaerobic process driven by the decomposition of organic material by methanogenic bacteria in the flooded soil conditions. The approach for these CH_4 emissions were directly sourced from the findings presented in Sahil et al.[18]. Nitrous Oxide (N_2O) emissions from the rice cultivation area were sourced from Sahil et al.[2] by accounting for both direct and indirect emission pathways. Direct emissions considered nitrogen inputs from several key sources:

the application of nitrogen-based fertilizers, the incorporation and decomposition of rice residues left in the field, and the cycling of nitrogen within the soil organic matter pool itself. Indirect emissions, which occur after nitrogen leaves the immediate site of application, were also included. These indirect pathways involve nitrogen loss through volatilization (ammonia transforming to N_2O elsewhere), leaching (nitrate moving through the soil profile and undergoing denitrification in anaerobic zones), and runoff (nitrogen compounds transported off-site and converted to N_2O). The specific dataset, methodologies and parameters utilized for calculating these direct and indirect N_2O emission components were taken from ref.[2].

Section S10 – Dynamic Season Identification

The calculation process involves first identifying the duration and timing of three rice growing seasons dynamically per financial year using satellite-derived flood and vegetation indices, specifically the LSWI, EVI, and NDVI. The onset of flooding is identified as the minimum annual ordinal date during the financial year (ordinal date = 0 for May 1st and 365 for May 31st), where the LSWI is greater than or equal to the EVI or NDVI indicating the presence of standing water or saturated surface conditions. The end dates for each of the three rice seasons are set based on transitions indicated by spectral indices after the onset of flooding. Specifically for the first season (S1), its end date is primarily identified as the earliest annual ordinal date where a return to flooded conditions (LSWI > NDVI or EVI) is detected, provided this detection occurs more than 80 days after the onset of initial flooding. This 80-day period is assigned to circumnavigate around consecutive flooding (typically rice field are dried before harvest) and get the onset of next season. Should no such return to flooded conditions be identified beyond this 80-day interval, the end date is assigned the 360th annual ordinal date. This default assignment is overridden if the date corresponding to the onset of initial flooding plus 120 days (maximum rice crop period in India) occurs before the 360th annual ordinal date, in which case the end date is set to the onset of initial flooding plus 120 days. The end dates for the second (S2) and third (S3) cultivation seasons are calculated using the identical methodology, applying the 80-day and 120-day interval criteria relative to the end date of the preceding rice season.

Section S11 – Synthetic Fertilizer Apportionment

This apportionment became necessary because direct rice-specific fertilizer use statistics were not available at the district level. The approach assumed that fertilizer allocation within a district is proportional to the area occupied by each crop type.

The percentage of each district's gross cropped area dedicated to rice cultivation was calculated from the ICRISAT dataset and multiplied by the district's total fertilizer use for each nutrient (N, P, K). Subsequently, this estimated rice-specific fertilizer amount was converted into an application rate (kg/ha) by dividing by the total rice cropped area within the district. This provided an estimate of the probable application rate of N, P, or K fertilizer specifically for rice cultivation within that district. The ICRISAT dataset's district-level fertilizer consumption data was geographically coded, based on 1966 administrative district boundaries (these historical boundaries are considerably larger than current district divisions due to subsequent administrative reorganizations). Consequently, the calculated district-level fertilizer application rates correspond to these 1966 districts. Lacking a 1966 vector map, a 1971 district shapefile was utilized as a proxy. This 1971 shapefile was found to have district boundaries identical to the 1966 boundaries (found through visual comparison on the website of ICRISAT data), making it the most suitable available option for geocoding the ICRISAT data. The calculated district fertilizer application rates for N, P, and K were then assigned as attribute values to the corresponding polygon features within this 1971 India district shapefile.

Following this, a geoprocessing workflow within ArcGIS 10.7.1 using Model Builder was employed to convert the vector dataset (the 1971 district shapefile with associated fertilizer application rate attributes) into a raster format. This rasterization process assigned the attribute value of each input polygon to all 500 *m* resolution pixels falling within that polygon's spatial extent, generating a continuous gridded representation of the estimated district-level application rates across the study area. The calculated fertilizer application rate (kg/ha) rasters were assigned specifically to the mapped rice cultivation areas within that district through clipping operation in ArcGIS 10.7.1. The outcome of this process is a gridded dataset depicting the estimated N, P, and K fertilizer application rates (kg/ha) for each 500 *m* rice pixel across India which was used for subsequent analyses.

Section S12 – Calculating Biomass for Crop Residue Return

Based on rice areas and yields, the initial step involved the segregation of rice areas that had undergone burning from those where residues remained unburned after harvesting. By overlaying the spatial information regarding burned areas from MODIS (MCD64A1.061) onto the locations where rice areas were mapped, we isolated the specific pixels where burning had not occurred, thereby creating a subset of data representing only unburned conditions. This process was important because the post-harvest management of crop residues, specifically whether they are combusted in the field or left to decompose or are incorporated into the soil, profoundly impacts the subsequent organic matter dynamics and nutrient cycling within the agricultural ecosystem, making it imperative to analyze these two distinct scenarios separately to accurately quantify biomass contributions in LCA.

Following this segregation, within the delineated unburned areas, the total biomass/residue produced was calculated, based on the mapped rice yield data and an established harvest index [2,18]. The harvest index (HI) is an agricultural metric, representing the ratio of grain yield to the total above-ground biomass produced by the crop. Using this ratio, an estimate of the entire above-ground biomass/residue, including stalks, leaves, and other vegetative parts, that was present at physiological maturity was obtained. Subsequently, the root to shoot ratio of rice was utilized to calculate the belowground biomass and then the total biomass by summing above and below ground biomass.

To further calculate residue returned, a specific assumption based on typical post-harvest fate of crops in the study region was applied to this calculated total biomass. This involved if only 5% of the above-ground biomass was returned to the soil, while the entire portion of the below-ground biomass, was considered to remain within the soil profile and decompose naturally. The assumption of a relatively low percentage return for above-ground biomass reflects common post-harvest practices in many Indian agricultural systems where the majority of stalks and leaves may be removed from the field for various purposes such as animal fodder, building material, or other off-farm uses, or may be partially lost through shattering and scattering during the harvesting process itself, leaving only a small fraction, such as the lower portion of the stubble, behind[5]. In contrast, the assumption of 100% return for below-ground biomass is standard in agricultural modeling because the root system naturally senesces and decomposes *in situ* after the crop matures and is harvested, thereby contributing its entire mass to the soil organic matter pool at the depth zone where the roots grew. The obtained residue from this process is then converted into carbon equivalents.

Section S13 – Pesticide Application Model Details

Due to the lack of fine-scale pesticide data, a machine learning model (random forest) was trained using national level data to predict national level pesticide application, crop yield, and fertilizer usage spanning from 2004 to 2021. These variables were selected based on the understanding that agricultural productivity (yield) is often correlated with fertilizer and pesticide use are frequently co-applied as part of integrated crop management strategies aimed at maximizing production and minimizing losses to pests and diseases. Higher yields often imply more intensive cultivation practices which typically involve increased use of both fertilizers to supply nutrients and pesticides to protect against biotic stresses. Similarly, increased fertilizer application, by promoting vigorous plant growth, can sometimes alter plant susceptibility to certain pests or diseases, potentially influencing pesticide requirements.

This training process allowed the model to learn the complex, non-linear relationships between national rice yield, national fertilizer application, and national pesticide use. To ensure the model's predictions were transferable across different scales, following steps were taken to achieve scale independence. First, due to the absence of crop-specific fertilizer data, the method used to apportion fertilizer application was similarly applied to pesticide application. Second, both the model's input features (yield and fertilizer) and its output (predicted pesticide application) were divided by the national rice areas. This normalization converted all relevant units to kg/ha, ensuring the model operated on intensity rather than absolute values to maintain scale independence. Following the successful development and validation (Table S4) of this national-level model predicting pesticide application in kg/ha, the subsequent phase involved using the model to generate predictions at a much finer 500 *m* resolution. Due to the aggregated nature of available consumption data and the variability in C-cost for individual pesticides, an average value of 4.93 kg C / kg pesticides, based on estimates by ref. [6], was employed in this study.

References

1. ICRISAT. International Crops Research Institute for the Semi-Arid Tropics (ICRISAT)-District Level Data. (2017).
2. Sahil, F. M., Narayanan, M. & Ilampooranan, I. Nitrous oxide emissions dynamics in Indian agricultural landscapes: Revised emission rates and new insights. *Agric. Ecosyst. Environ.* **356**, 108639 (2023).
3. Kimura, S. D., Mishima, S.-I. & Yagi, K. Carbon resources of residue and manure in Japanese farmland soils. *Nutr. Cycl. Agroecosystems* **89**, 291–302 (2011).
4. Narayanan, M., Sharma, A. & Ilampooranan, I. Spatio-temporally Explicit Decoupling of Rice Yield and Methane Emission Relationships in India. *SSRN Electron. J.* https://dx.doi.org/10.2139/ssrn.5781084 (2025) doi:https://dx.doi.org/10.2139/ssrn.5781084.
5. Bhatia, A., Jain, N. & Pathak, H. Methane and nitrous oxide emissions from Indian rice paddies, agricultural soils, and crop residue burning. *Greenh. Gases Sci. Technol.* **3**, 356–371 (2013).
6. West, T. O. & Marland, G. A synthesis of carbon sequestration, carbon emissions, and net carbon flux in agriculture: comparing tillage practices in the United States. *Agric. Ecosyst. Environ.* **91**, 217–232 (2002).
7. Benbi, D. K. Carbon footprint and agricultural sustainability nexus in an intensively cultivated region of Indo-Gangetic Plains. *Sci. Total Environ.* **644**, 611–623 (2018).
8. Verkaik, J., Sutanudjaja, E. H., Oude Essink, G. H. P., Lin, H. X. & Bierkens, M. F. P. GLOBGM v1.0: a parallel implementation of a 30\,arcsec PCR-GLOBWB-MODFLOW global-scale groundwater model. *Geosci. Model Dev.* **17**, 275–300 (2024).
9. Nelson, G. C. *et al. Greenhouse Gas Mitigation: Issues for Indian Agriculture*. (Intl Food Policy Res Inst, 2009).
10. Bouman, B. Examining the water-shortage problem in rice systems: Water-saving irrigation technologies. in *Rice Science: Innovations and Impact for Livelihood. Proceedings of the International Rice Research Conference* 519–535 (International Rice Research Institute (IRRI), Beijing, China, 2003).
11. Surendhar, M., Anbuselvam, Y. & Ivin, J. J. S. Status of rice cultivation under Indian saline lowlands. *J. Pharmacogn. Phytochem.* **10**, 371–376 (2021).
12. Agriculture Census Division, Department of Agriculture & Cooperation. *Input Survey 2011-12: Manual of Schedules and Instructions for Data Collection*. (Ministry of Agriculture, Government of India, New Delhi, 2011).
13. Intergovernmental Panel on Climate Change (IPCC). Chapter 5: Croplands. in *2006 IPCC Guidelines for National Greenhouse Gas Inventories* 1–54 (IPCC, 2006).
14. Ravindra, K. *et al.* Real-time monitoring of air pollutants in seven cities of North India during crop residue burning and their relationship with meteorology and transboundary movement of air. *Sci. Total Environ.* **690**, 717–729 (2019).
15. Montes, C., Sapkota, T. & Singh, B. Seasonal patterns in rice and wheat residue burning and surface PM2.5 concentration in northern India. *Atmospheric Environ. X* **13**, 100154 (2022).
16. Gadde, B., Bonnet, S., Menke, C. & Garivait, S. Air pollutant emissions from rice straw open field burning in India, Thailand and the Philippines. *Environ. Pollut.* **157**, 1554–1558 (2009).
17. Andreae, M. O. & Merlet, P. Emission of trace gases and aerosols from biomass burning. *Glob. Biogeochem. Cycles* **15**, 955–966 (2001).
18. Sahil, F. M., Narayanan, M. & Ilampooranan, I. Setting Up Methane Mitigation Measures for Indian Rice Fields: Representative Emissions and New Interpretations. *Glob. Biogeochem. Cycles* **38**, e2024GB008107 (2024).

Figures

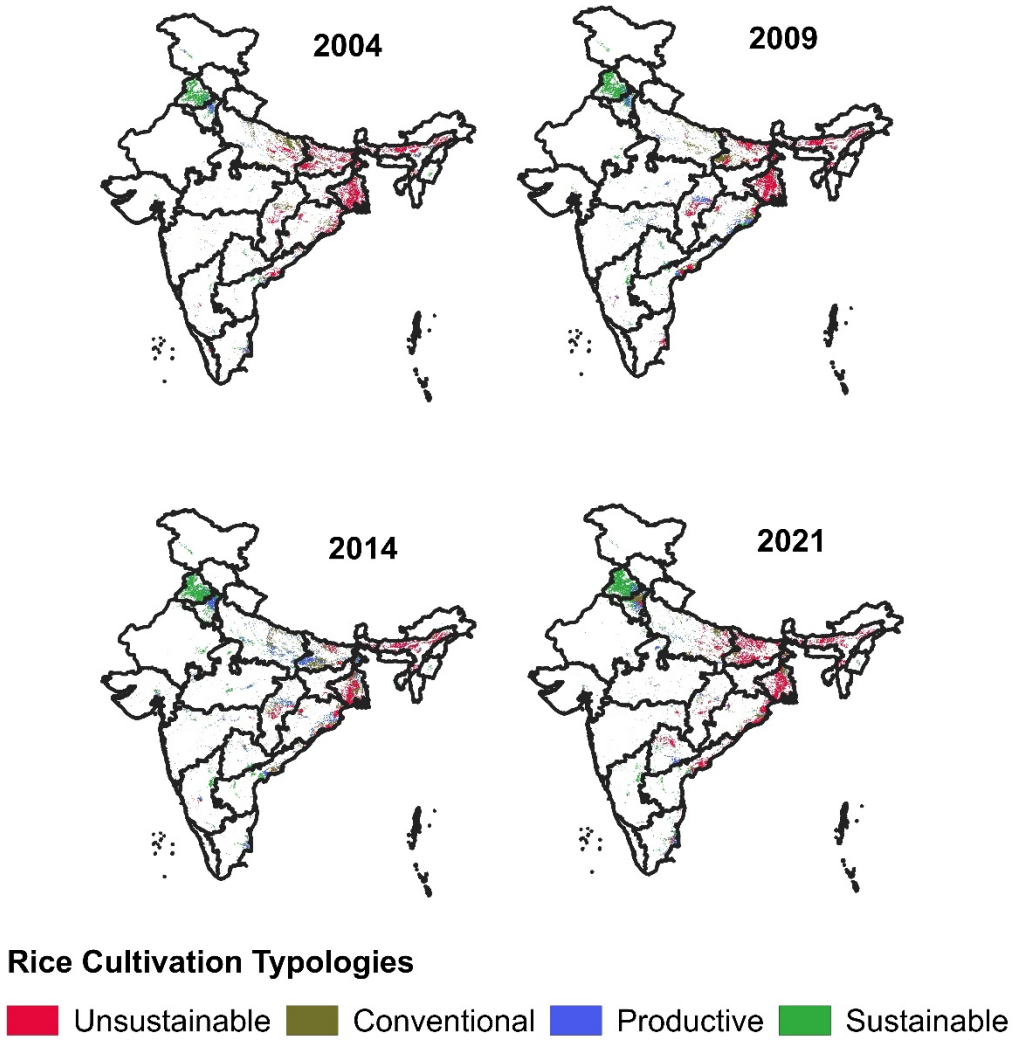

Figure S1: Shifts in rice cultivation typologies from 2004 to 2021

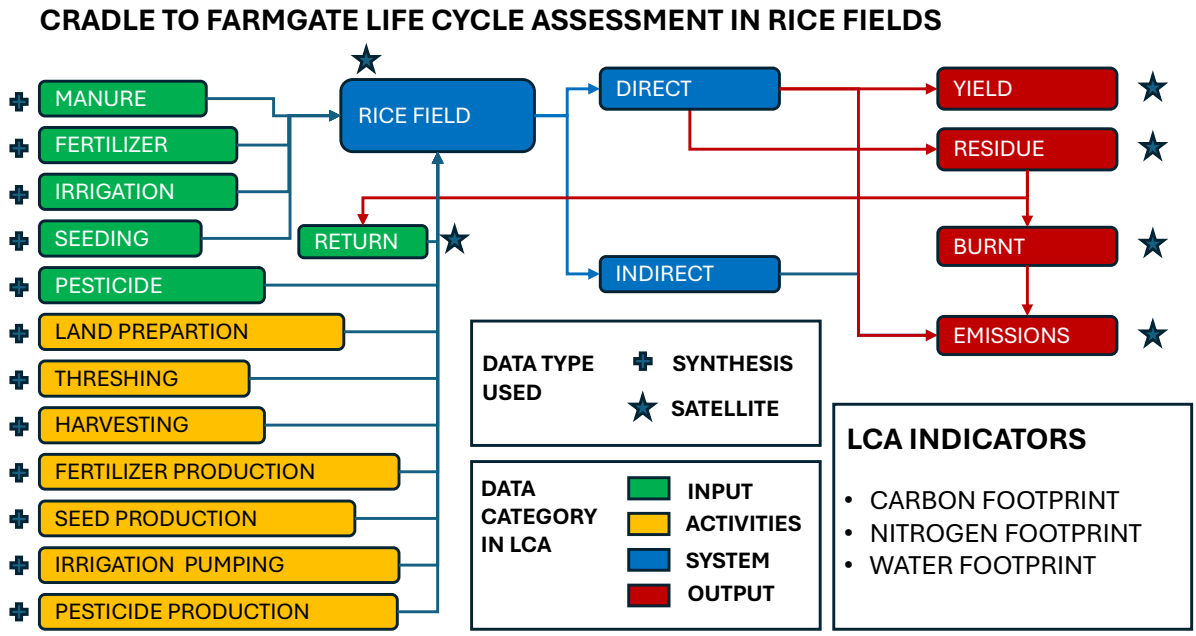

Figure S2: Components of satellite-based life cycle assessment (cradle to farmgate)

Figure S2: Carbon Inputs, outputs, and activities of the Rice LCA in India.

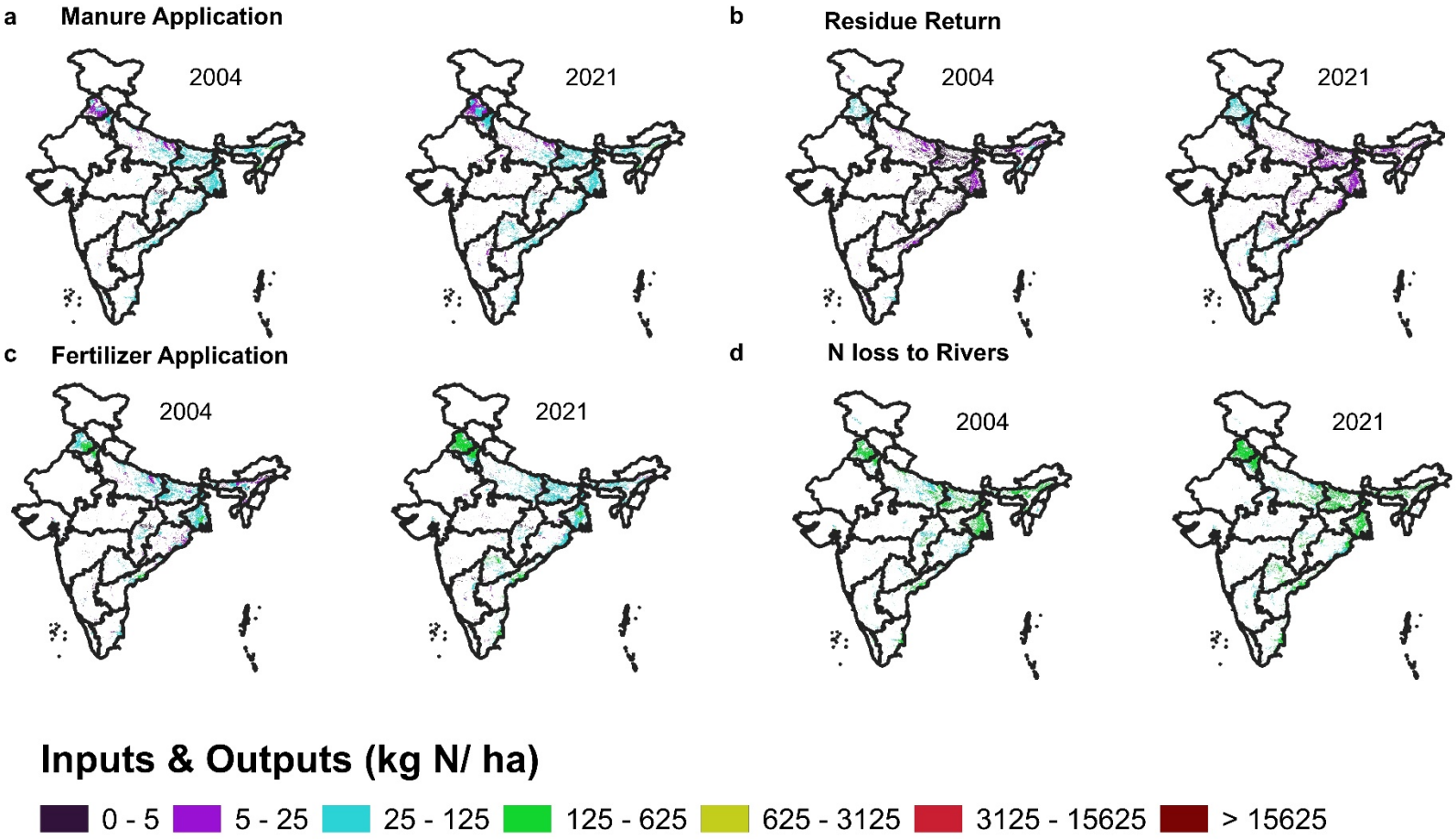

Figure S3: Nitrogen Inputs and Outputs of the Rice LCA in India.

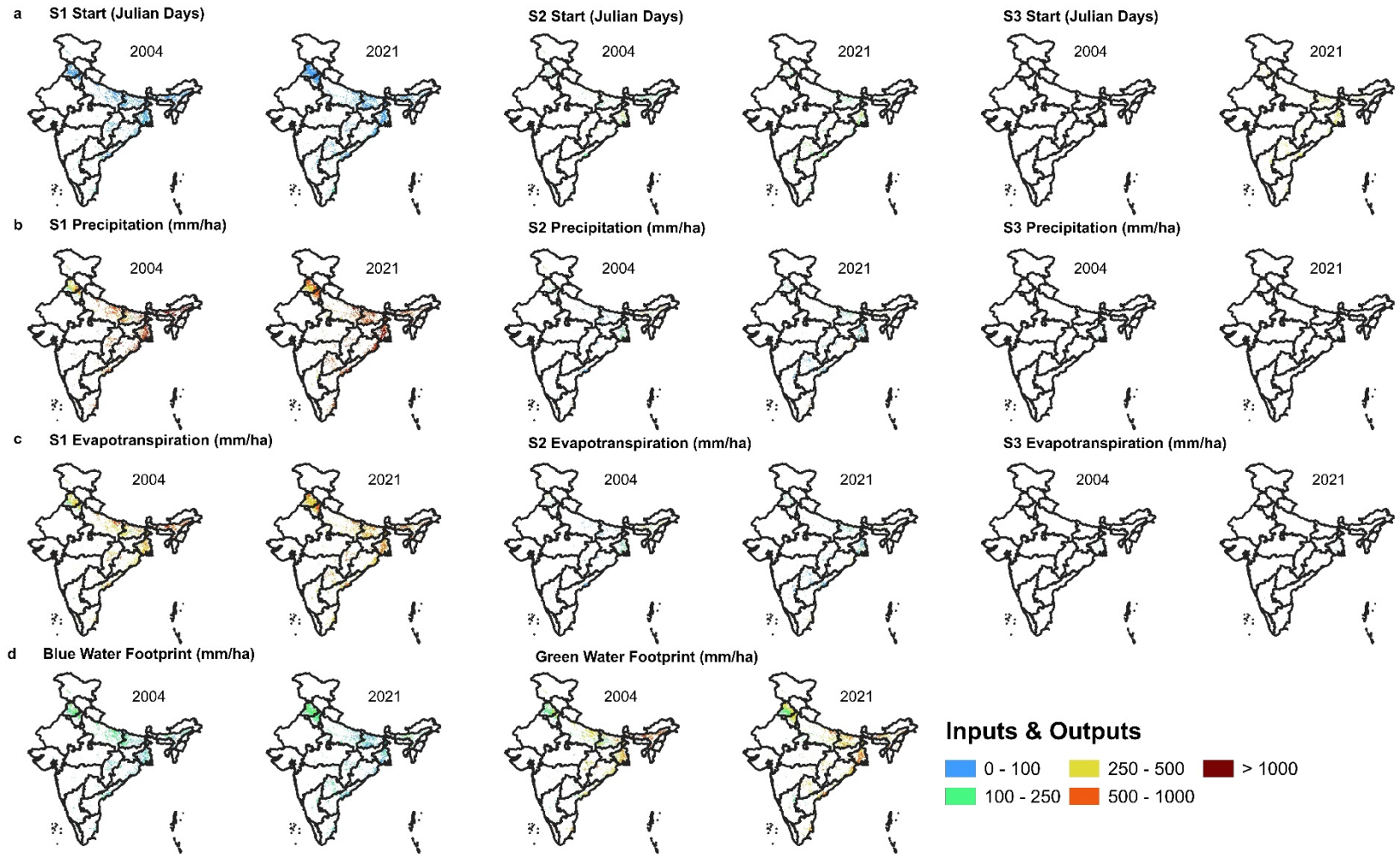

Figure S4: Water Inputs and Outputs of the Rice LCA in India.

Tables

Table S1: Average LCA indicator values per region

Region	LCA Indicator	2004	2021
Andhra	Carbon Footprint (kg C / ha)	709 (-363-1674)	675 (-255-4057)
	Nitrogen Footprint (kg N / ha)	132 (108-156)	144 (107-173)
	Rice Yield (kg C / ha)	553 (56-1808)	916 (37-1066)
	Water Footprint (mm / ha)	413 (1-908)	485 (1-1091)
Bengal	Carbon Footprint (kg C / ha)	1199 (-990-24785)	1331 (-155-23519)
	Nitrogen Footprint (kg N / ha)	133 (107-211)	139 (107-231)
	Rice Yield (kg C / ha)	317 (12-1990)	434 (30-1662)
	Water Footprint (mm / ha)	575 (7-1685)	577 (3-1588)
Punjab	Carbon Footprint (kg C / ha)	2304 (-1876-97594)	2443 (-1729-82867)
	Nitrogen Footprint (kg N / ha)	136 (107-154)	149 (107-175)
	Rice Yield (kg C / ha)	1450 (314-2277)	1639 (368-2475)
	Water Footprint (mm / ha)	392 (13-1418)	476 (11-1149)

Table S2: Percentage distribution of cultivation typologies' persistence classes in rice areas

Persistence Class	Persistence Level	Unsustainable	Conventional	Productive	Sustainable
Non-Persistent	Very Low (0.0-0.2)	54.36%	76.34%	82.24%	71.42%
	Low (0.2-0.4)	20.04%	19.07%	14.29%	11.70%
Moderate	Moderate (0.4-0.6)	9.57%	4.08%	2.90%	3.97%
Persistent	High (0.6-0.8)	9.87%	0.52%	0.57%	5.09%
	Very High (0.8-1.0)	6.16%	0.00%	0.00%	7.82%

Table S3: Yield footprints, Trade Value (in Billion USD) and number of countries with high footprints under each typology transition

	Years	2004	2005	2006	2007	2008	2009	2010	2011	2012	2013	2014	2015	2016	2017	2018	2019	2020	2021
Footprint Use Efficiency[#]	Base Case	0.52	0.67	0.73	0.72	0.64	0.69	0.86	0.89	0.75	0.93	0.89	1.01	0.70	1.01	0.97	0.98	0.71	0.81
	Unsustainable	0.34	0.54	0.61	0.52	0.31	0.48	0.72	0.70	0.44	0.73	0.77	0.63	0.38	0.74	0.79	0.76	0.43	0.41
	Conventional	0.23	0.39	0.68	0.54	0.37	0.47	0.53	0.70	0.50	0.62	0.69	0.57	0.57	0.85	0.90	0.82	0.47	0.52
	Productive	0.43	0.61	0.47	0.64	0.54	0.62	0.76	1.13	0.87	1.17	1.08	1.17	0.82	1.21	1.00	1.05	0.73	0.99
	Sustainable	1.23	1.34	1.35	1.34	1.33	1.39	1.32	1.34	1.21	1.35	1.23	1.41	1.19	1.54	1.44	1.43	1.17	1.31
Trade Value (Billion USD)	Base Case	1.18	1.64	1.46	2.35	2.84	2.40	2.30	4.07	6.13	8.17	7.91	6.38	5.32	7.08	7.35	6.80	7.98	9.62
	Unsustainable	0.76	1.32	1.23	1.70	1.38	1.68	1.92	3.23	3.58	6.36	6.86	3.96	2.86	5.17	6.01	5.23	4.79	4.92
	Conventional	0.51	0.95	1.37	1.77	1.65	1.64	1.40	3.20	4.07	5.44	6.12	3.62	4.32	5.94	6.83	5.70	5.24	6.16
	Productive	0.98	1.47	0.94	2.08	2.38	2.15	2.01	5.17	7.14	10.22	9.60	7.36	6.19	8.45	7.59	7.29	8.21	11.76
	Sustainable	2.78	3.26	2.71	4.36	5.86	4.82	3.51	6.15	9.94	11.86	10.93	8.92	9.01	10.80	10.94	9.87	13.08	15.59
Number of High Footprints Countries (upper 5%[*])	Base Case	4	4	3	3	3	3	2	3	7	4	8	7	8	9	7	5	12	16
	Unsustainable	4	4	3	4	3	3	2	4	11	5	7	9	11	10	7	5	17	21
	Conventional	6	5	4	4	3	3	3	4	8	7	8	9	10	10	8	6	17	19
	Productive	4	3	3	3	3	2	2	3	5	4	4	4	8	5	5	2	12	11
	Sustainable	1	0	0	1	1	0	0	0	1	3	0	0	0	0	0	1	4	5

[#]Refer to Methods Section Export Flow Analysis for definition and formula

[*]Upper 5% represents countries having nitrogen footprint >29 thousand tons, carbon footprint >0.33 million tons, and water footprint >1066 MCM

Table S4: Pesticide and Seed Application Model Accuracies

Estimated Variable	Model Name	Best Hyperparameters	Training R2	Testing R2
Pesticide	Linear Regression	Default	0.11	-0.56
	Polynomial Model (Excel Trained)	Default	0.79	**0.79**
	Random Forest	n_estimators: 140,max_depth: 32,min_samples_split: 3,min_samples_leaf: 2	0.87	0.68
	Support Vector Machine (SVR)	kernel: 'rbf',C: 999.84,epsilon: 2.37,gamma: 'scale'	0.42	0.34
	Neural Network (MLP)	hidden_layer_sizes: 132,activation: 'relu',solver: 'lbfgs',alpha: 1.49e-05	-2.13	0.68
	Gradient Tree Boost (XGB)	n_estimators: 51,max_depth: 5,learning_rate: 0.057,subsample: 0.602,colsample_bytree: 0.894	0.93	0.72
Seeding	Linear Regression (Excel Trained)	Default Parameters	**0.29**	0.29
	Polynomial Model (Excel Trained)	Default	0.39	-0.33
	Random Forest	n_estimators: 53, max_depth: 2, min_samples_split: 2, min_samples_leaf: 7	0.00	-120.63
	Support Vector Machine (SVM)	kernel: 'sigmoid', C: 13.043, epsilon: 4.609, gamma: 'scale'	-0.12	-151.67
	Neural Network (MLP)	hidden_layer_sizes: 422, activation: 'logistic', solver: 'adam', alpha: 0.0618	0.02	-120.63
	Gradient Tree Boost (GTB)	n_estimators: 52, max_depth: 15, learning_rate: 0.0105, subsample: 0.944, colsample_bytree: 0.617	0.45	-134.94

Table S5: Classification thresholds for NMIS Rasters

Typology	Quartile	NMIS Range
Unsustainable	Q1	NMIS ≤ -0.1552
Conventional	Q2	-0.1552 < NMIS ≤ -0.0952
Productive	Q3	-0.0952 < NMIS ≤ -0.0325
Sustainable	Q4	NMIS > -0.0325

Table S6: Forecast model hyperparameter details

Model Name	Hyperparameter Name	Hyperparameter Definition	Hyperparameter Range
Support Vector Machines	kernel	Specifies the kernel type to be used in the algorithm	['rbf', 'poly', 'linear']
	C	Regularization parameter (inverse of regularization strength)	1e-2 to 1e3 (log)
	epsilon	Epsilon-tube within which no penalty is associated in the training loss function	1e-4 to 1e-1 (log)
	gamma	Kernel coefficient for 'rbf'	1e-4 to 1e1 (log)
	degree	Degree of the polynomial kernel function	2 to 5
Decision Tree	criterion	The function to measure the quality of a split	['squared_error', 'friedman_mse', 'absolute_error']
	splitter	The strategy used to choose the split at each node	['best', 'random']
	max_depth	The maximum depth of the tree	2 to 32
	min_samples_split	The minimum number of samples required to split an internal node	2 to 20
	min_samples_leaf	The minimum number of samples required to be at a leaf node	1 to 20
Random Forest	n_estimators	The number of trees in the forest	50 to 500
	criterion	The function to measure the quality of a split	['squared_error', 'absolute_error']
	max_depth	The maximum depth of the tree	2 to 32 (log)
	min_samples_split	The minimum number of samples required to split an internal node	2 to 20
	min_samples_leaf	The minimum number of samples required to be at a leaf node	1 to 20
	max_features	The number of features to consider when looking for the best split	['sqrt', 'log2', None]
	bootstrap	Whether bootstrap samples are used when building trees	[True, False]
Extreme Gradient Boosting	booster	Which booster to use (tree-based models)	['gbtree', 'dart']
	n_estimators	Number of gradient boosted trees	50 to 500
	max_depth	Maximum tree depth for base learners	2 to 10
	learning_rate	Boosting learning rate (step size shrinkage)	0.01 to 0.3 (log)
	subsample	Subsample ratio of the training instances	0.5 to 1.0
	colsample_bytree	Subsample ratio of columns when constructing each tree	0.5 to 1.0

Model Name	Hyperparameter Name	Hyperparameter Definition	Hyperparameter Range
	gamma	Minimum loss reduction required to make a further partition on a leaf node	1e-8 to 1.0 (log)
	reg_alpha	L1 regularization term on weights	1e-8 to 1.0 (log)
	reg_lambda	L2 regularization term on weights	1e-8 to 1.0 (log)
Neural Network	optimizer	Optimization algorithm used to update weights	['adam', 'rmsprop']
	learning_rate	Learning rate for the optimizer	1e-4 to 1e-1 (log)
	n_layers	Number of dense hidden layers	1 to 100
	n_units	Number of neurons per hidden layer	4 to 16 (log)
	activation	Activation function for hidden layers	['relu', 'tanh']
	epochs	Number of training epochs	30 to 150
	batch_size	Number of samples per gradient update	[2, 4, 8, 16]
Long Short Term Memory	optimizer	Optimization algorithm used to update weights	['adam', 'rmsprop']
	learning_rate	Learning rate for the optimizer	1e-4 to 1e-1 (log)
	epochs	Number of training epochs	30 to 150
	batch_size	Number of samples per gradient update	[8, 16]
	lstm_units	Dimensionality of the LSTM output space	8 to 64 (log)
	activation	Activation function for the LSTM layer	['relu', 'tanh']
Transformer	optimizer	Optimization algorithm used to update weights	['adam', 'rmsprop']
	learning_rate	Learning rate for the optimizer	1e-4 to 1e-1 (log)
	epochs	Number of training epochs	30 to 150
	batch_size	Number of samples per gradient update	[8, 16]
	head_size	Key dimension size for MultiHeadAttention	8 to 32 (log)
	num_heads	Number of attention heads	2 to 4
	ff_dim	Dimensionality of the feed-forward network	4 to 32 (log)
	num_transformer_blocks	Number of stacked transformer layers	1 to 4
	dropout	Dropout rate for regularization	0.0 to 0.1

Table S7: Forecast model performance for each typology (bolded indicator selected model in each typology)

Typology	Model	Train NSE	Validation NSE	Best Objective Score	Best Parameters
Unsustainable	ARIMA	0.0942	-2.1492		
Unsustainable	Linear Regression	0.271	-0.8012		
Unsustainable	Support Vector Machines	0.1398	0.0806	0.051	{'kernel': 'poly', 'C': 0.3865142850555638, 'epsilon': 0.005412102629650287, 'degree': 4}
Unsustainable	Decision Tree	0	-0.0114	-0.0171	{'criterion': 'friedman_mse', 'splitter': 'random', 'max_depth': 25, 'min_samples_split': 18, 'min_samples_leaf': 2}
Unsustainable	Random Forest	-0.0001	-0.0133	-0.009	{'n_estimators': 424, 'criterion': 'squared_error', 'max_depth': 15, 'min_samples_split': 16, 'min_samples_leaf': 6, 'max_features': 'log2', 'bootstrap': True}
Unsustainable	Extreme Gradient Boosting	0.0127	-0.0026	-0.0103	{'booster': 'gbtree', 'n_estimators': 241, 'max_depth': 7, 'learning_rate': 0.015708164027557585, 'subsample': 0.5439645716152642, 'colsample_bytree': 0.8777667659744737, 'gamma': 4.641486399357559e-06, 'reg_alpha': 0.3405586477505312, 'reg_lambda': 0.00031028434462138804}
Unsustainable	**Neural Network**	**0.937**	**0.7437**	**0.825**	**{'optimizer': 'rmsprop', 'learning_rate': 0.04609420019532739, 'n_layers': 1, 'n_units': 4, 'activation': 'tanh', 'epochs': 110, 'batch_size': 8}**

Typology	Model	Train NSE	Validation NSE	Best Objective Score	Best Parameters
Unsustainable	LSTM	0.6318	0.1619	0.2918	{'optimizer': 'adam', 'learning_rate': 0.006602343101668675, 'epochs': 36, 'batch_size': 8, 'lstm_units': 20, 'activation': 'relu'}
Unsustainable	Transformer	-0.017	-0.0067	-0.0047	{'optimizer': 'adam', 'learning_rate': 0.00015587749069528398, 'epochs': 36, 'batch_size': 8, 'head_size': 16, 'num_heads': 4, 'ff_dim': 9, 'num_transformer_blocks': 3, 'dropout': 0.008179722747183194}
Conventional	ARIMA	-0.1676	-0.0093		
Conventional	Linear Regression	0.197	-0.4381		
Conventional	Support Vector Machines	0.6129	0.5932	0.5834	{'kernel': 'rbf', 'C': 396.13949540706335, 'epsilon': 0.0038164772908046503, 'gamma': 0.05128599825998754}
Conventional	Decision Tree	0.2703	0.2438	0.2306	{'criterion': 'absolute_error', 'splitter': 'best', 'max_depth': 13, 'min_samples_split': 8, 'min_samples_leaf': 5}
Conventional	Random Forest	0.7237	0.5464	0.4578	{'n_estimators': 274, 'criterion': 'absolute_error', 'max_depth': 8, 'min_samples_split': 5, 'min_samples_leaf': 1, 'max_features': None, 'bootstrap': False}

Typology	**Model**	**Train NSE**	**Validation NSE**	**Best Objective Score**	**Best Parameters**
Conventional	Extreme Gradient Boosting	0.3248	0.221	0.169	{'booster': 'gbtree', 'n_estimators': 375, 'max_depth': 7, 'learning_rate': 0.09122499437864785, 'subsample': 0.88573772253166, 'colsample_bytree': 0.5044237238476388, 'gamma': 0.0011041469411591624, 'reg_alpha': 1.7100270588589982e-05, 'reg_lambda': 7.111775998603911e-05}
Conventional	Neural Network	0.3236	0.192	0.322	{'optimizer': 'adam', 'learning_rate': 0.00031076485559138886, 'n_layers': 59, 'n_units': 15, 'activation': 'tanh', 'epochs': 137, 'batch_size': 2}
Conventional	**LSTM**	**0.5162**	**0.5099**	**0.5191**	**{'optimizer': 'rmsprop', 'learning_rate': 0.006222780757450897, 'epochs': 121, 'batch_size': 8, 'lstm_units': 51, 'activation': 'tanh'}**
Conventional	Transformer	0.0343	-0.0467	-0.0044	{'optimizer': 'adam', 'learning_rate': 0.00013090128915417494, 'epochs': 65, 'batch_size': 16, 'head_size': 22, 'num_heads': 4, 'ff_dim': 6, 'num_transformer_blocks': 3, 'dropout': 0.09517822181434309}
Productive	ARIMA	0.5957	-0.7408		
Productive	Linear Regression	0.5822	-1.486		

Typology	Model	Train NSE	Validation NSE	Best Objective Score	Best Parameters
Productive	Support Vector Machines	0.1123	0.1436	0.0967	{'kernel': 'poly', 'C': 0.11691543503113958, 'epsilon': 0.00022758722665094193, 'degree': 4}
Productive	Decision Tree	0	-0.0015	-0.0022	{'criterion': 'squared_error', 'splitter': 'best', 'max_depth': 7, 'min_samples_split': 18, 'min_samples_leaf': 5}
Productive	Random Forest	-0.0007	-0.0001	-0.0004	{'n_estimators': 93, 'criterion': 'absolute_error', 'max_depth': 20, 'min_samples_split': 13, 'min_samples_leaf': 8, 'max_features': 'log2', 'bootstrap': True}
Productive	Extreme Gradient Boosting	0	-0.0015	-0.0022	{'booster': 'gbtree', 'n_estimators': 56, 'max_depth': 7, 'learning_rate': 0.010040407582564404, 'subsample': 0.7262346344120854, 'colsample_bytree': 0.6337158148144565, 'gamma': 0.8505688586404251, 'reg_alpha': 0.7178272708601159, 'reg_lambda': 0.00045154233647396065}
Productive	Neural Network	0	-0.0016	-0.0005	{'optimizer': 'adam', 'learning_rate': 0.09683817428508339, 'n_layers': 19, 'n_units': 11, 'activation': 'relu', 'epochs': 133, 'batch_size': 4}

Typology	Model	Train NSE	Validation NSE	Best Objective Score	Best Parameters
Productive	LSTM	0.1334	0.0249	0.1422	{'optimizer': 'rmsprop', 'learning_rate': 0.0030449666250168235, 'epochs': 69, 'batch_size': 8, 'lstm_units': 20, 'activation': 'relu'}
Productive	Transformer	0.0036	-0.0105	0.0007	{'optimizer': 'rmsprop', 'learning_rate': 0.05364511361251952, 'epochs': 122, 'batch_size': 16, 'head_size': 23, 'num_heads': 3, 'ff_dim': 13, 'num_transformer_blocks': 3, 'dropout': 0.046749444482183954}
Sustainable	**ARIMA**	**0.2016**	**0.2712**		
Sustainable	Linear Regression	0.3004	0.1691		
Sustainable	Support Vector Machines	0.2802	0.2812	0.2797	{'kernel': 'linear', 'C': 2.325422705344265, 'epsilon': 0.06989383444367672}
Sustainable	Decision Tree	0.8776	-0.0596	0.5163	{'criterion': 'friedman_mse', 'splitter': 'best', 'max_depth': 24, 'min_samples_split': 4, 'min_samples_leaf': 2}
Sustainable	Random Forest	-0.0091	-0.0112	-0.0104	{'n_estimators': 128, 'criterion': 'absolute_error', 'max_depth': 4, 'min_samples_split': 17, 'min_samples_leaf': 18, 'max_features': 'sqrt', 'bootstrap': True}

Typology	Model	Train NSE	Validation NSE	Best Objective Score	Best Parameters
Sustainable	Extreme Gradient Boosting	0.9994	0.6263	0.4398	{'booster': 'dart', 'n_estimators': 54, 'max_depth': 9, 'learning_rate': 0.19163155562140907, 'subsample': 0.7716685524956935, 'colsample_bytree': 0.7272047839248154, 'gamma': 3.6423997980117665e-06, 'reg_alpha': 4.922323484921045e-07, 'reg_lambda': 4.6765571512405045e-05}
Sustainable	Neural Network	0.6816	0.3933	0.4076	{'optimizer': 'adam', 'learning_rate': 0.00015191051995275265, 'n_layers': 67, 'n_units': 15, 'activation': 'tanh', 'epochs': 30, 'batch_size': 2}
Sustainable	LSTM	-0.0279	-0.0023	0.0104	{'optimizer': 'rmsprop', 'learning_rate': 0.0001692355594032883, 'epochs': 47, 'batch_size': 16, 'lstm_units': 19, 'activation': 'relu'}
Sustainable	Transformer	0.1326	-0.0125	0.0097	{'optimizer': 'adam', 'learning_rate': 0.00011724351963289054, 'epochs': 115, 'batch_size': 16, 'head_size': 21, 'num_heads': 2, 'ff_dim': 16, 'num_transformer_blocks': 2, 'dropout': 0.04114084349395633}

3